Kennisprogramma Natte Kunstwerken
Kennisplan 2024

Vervangings- en renovatieopgave
natte kunstwerken in Nederland

Kennisbijdrage:

Einde levensduur overige HWS-objecten

Remaining service life prediction of concrete structures in marine environments

Chloride induced corrosion

Auteurs
H.J.J. Weijs (TNO)
G.A. Torres-Alves (TNO)
Raphaël Steenbergen (TNO)
Henco Burggraaf (TNO)

kenmerk : KpNK-2023-KV1.3-kunstwerk-a007
versie : 1.0
datum publicatie : 14 november 2023

Voorwoord

Kennisprogramma Natte Kunstwerken

Sluizen, stuwen, gemalen en stormvloedkeringen zijn belangrijke assets waarvoor beheerders zoals Rijkswaterstaat en de waterschappen verantwoordelijk zijn. Veel van deze natte kunstwerken in de waterinfrastructuur bereiken de komende decennia het einde van hun (technische en/of functionele) levensduur. Zij kunnen daardoor hun functies naar verwachting niet meer adequaat blijven uitoefenen. Dit zal ten koste gaan van de mate waarin de waterinfrastructuur voldoet aan betrouwbaarheidseisen. In het kader van goed assetmanagement staan we dan ook voor de enorme opgave om deze kunstwerken te vervangen of te renoveren. Welke kennis hebben we nodig om dat efficiënt, kostenbesparend en toekomst-bestendig aan te pakken?

In het Kennisprogramma Natte Kunstwerken (KpNK) ontwikkelen en bundelen Deltares, MARIN, Rijkswaterstaat en TNO deze kennis op basis van de Samenwerkingsovereenkomst Natte Kunstwerken.

Werkwijze vervangings- en renovatieproces

De laatste jaren richten we ons niet meer uitsluitend op een-op-een vervanging van kunstwerken. We zoeken steeds meer naar mogelijkheden om hun levensduur te verlengen en (noodzakelijke) ingrepen te koppelen aan gebieds- en netwerkontwikkelingen en aan functionele ontwikkelingen. Rijkswaterstaat heeft als assetmanager een vernieuwde werkwijze voor dit vervangings- en renovatie-proces (VenR) opgesteld om een uniform en systematisch proces te hebben waarmee een VenR-maatregel transparant onderbouwd kan worden (zie Figuur 1).

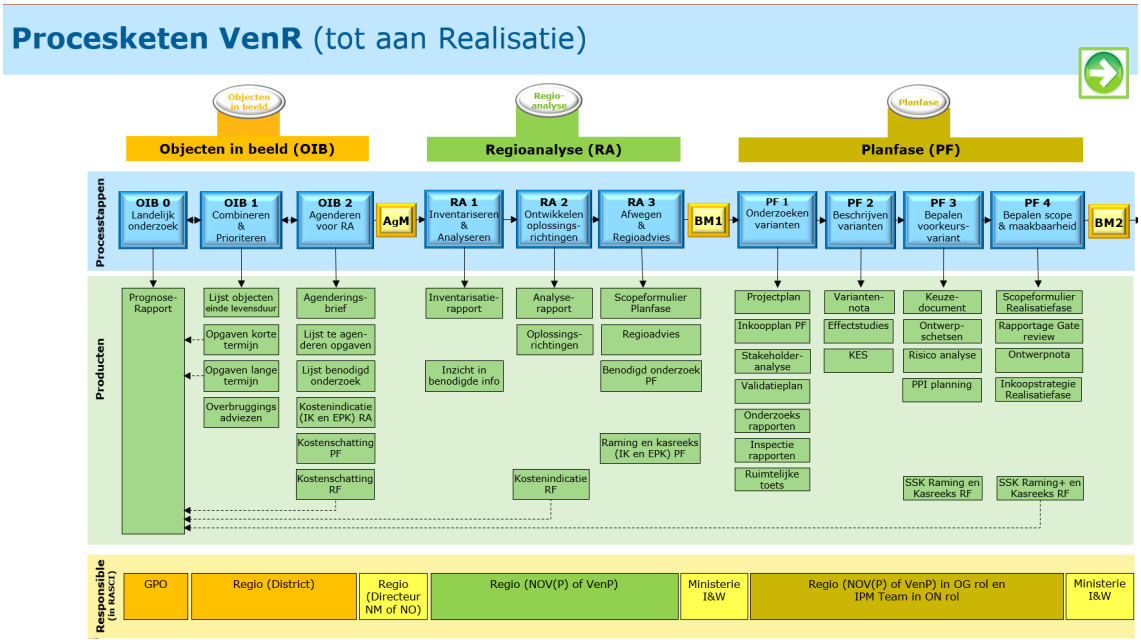

Figuur 1: Procesketen VenR binnen Rijkswaterstaat

Deze procesketen vormt de basis waar de kennisontwikkeling van het kennisprogramma aan bijdraagt.

Twee-stappen-benadering en drie kernvragen

De kennis die we ontwikkelen binnen het Kennisprogramma Natte Kunstwerken draagt bij aan de stapsgewijze-benadering binnen deze Procesketen VenR:

- stap 1 (*Objecten in Beeld*): richt zicht op (het einde van) de technische levensduur van een kunstwerk en het agenderen van de VenR-opgave in het *Prognoserapport*;
- stap 2 (*Regioanalyse*): brengt vooral de relatie in kaart tussen het kunstwerk en de netwerken waar het (samen met andere kunstwerken) deel van uitmaakt. In het resulterende *Regioadvies* gaat het ook over (het einde van) de functionele levensduur.

Inhoudelijk vindt het onderzoek plaats aan de hand drie *kernvragen*:

1. Hoe lang gaat mijn kunstwerk nog mee, zowel technisch als functioneel?
2. Welke alternatieven heb ik, behalve een-op-een vervanging?
3. Hoe weeg ik de alternatieven tegen elkaar af?

Programmaplan, jaarlijkse kennisplannen en samenwerking

Het programmaplan omvat de achtergronden en ambities voor de gehele looptijd van het Kennisprogramma Natte Kunstwerken. Jaarlijks worden deze ambities uitgewerkt in een kennisplan en een bijbehorend financieringsplan. Andere partijen, zoals waterschappen, adviesbureaus en andere (commerciële) organisaties, nodigen we uitdrukkelijk uit om deel te nemen aan het gezamenlijk uitvoeren van een kennisplan, bijvoorbeeld met kennisbijdragen in voor hen relevante onderzoeksprojecten, met praktijkervaringen of financiële bijdragen.

Resultaten delen

Bijdragen en onderzoeksresultaten uit ons Kennisprogramma Natte Kunstwerken delen we met de hele sector via onze website (www.nattekunstwerkenvandetoekomst.nl) en op andere manieren.

Hieronder vindt u een kennisbijdrage binnen werkpakket ‘Einde levensduur overige HWS-objecten’ uit het Kennisplan 2024. Het omvat eerst de samenvatting van het onderzoek ‘Degradation of concrete structures in marine environments’. Deze activiteit is namens het Kennisprogramma Natte Kunstwerken geleid door TNO. Na de samenvatting vindt u het volledige onderzoeksverslag in de vorm van een onderzoeksrapport.

N.B. Het volledige onderzoeksrapport is gelijk aan het originele onderzoeksrapport van TNO, met uitzondering van het titelblad en de technische samenvatting. Bij publicatie van dit onderzoeks-verslag op de KpNK-website is het titelblad om privacyredenen verwijderd. En een meer toegankelijke samenvatting volgt hierna.

Meer informatie

- Het Kennisprogramma Natte Kunstwerken is de uitwerking van de onderzoekslijn 'Toekomstbestendige Natte Kunstwerken' binnen het Nationaal Kennisplatform voor Water en Klimaat (NKWK). Zie www.waterenklimaat.nl

- Voor meer informatie over het programma Kennisprogramma Natte Kunstwerken, zie www.nattekunstwerkenvandetoekomst.nl.

- Voor vragen over het Kennisprogramma Natte Kunstwerken en het kennisplan 2024 kunt u terecht bij Martine Brinkhuis, email martine.brinkhuis@rws.nl

- Voor vragen over de voorliggende kennisbijdrage kunt u terecht bij de auteurs:

H.J.J. Weijs (TNO) harrie.weijs@tno.nl

G.A. Torres-Alves (TNO) gina.torres-alves@tno.nl

Samenvatting

Einde levensduur overige HWS-objecten

Remaining service life prediction of concrete structures in marine environments

Chloride induced corrosion

Hieronder vindt u een kennisbijdrage van het werkpakket 'Einde levensduur overige HWS-objecten' uit het Kennisplan 2024. De bijdrage – geleid door TNO – omvat de samenvatting van het onderzoek 'Remaining service life prediction of concrete structures in marine environments'. Na de samenvatting vindt u het volledige rapport.

Aanleiding en probleemstelling

Een groot deel van Nederland is kwetsbaar voor overstromingen. Ruim een kwart van het land ligt onder zeeniveau en nog eens een derde is direct afhankelijk van het functioneren van de waterkeringen. Deze keringen omvatten onder andere dijken, dammen, stormvloedkeringen en andere waterregulerende kunstwerken. Het functioneren van de stormvloedkeringen en kunstwerken is niet alleen essentieel voor de waterveiligheid, maar ook voor de waterhuishouding en voor de scheepvaart. De economische waarde is dus groot.

Veel van deze kunstwerken zijn in de tweede helft van de twinstige eeuw gebouwd en daarmee verouderd. Omdat de beoogde levensduur van 75 jaar nadert is er dringend behoefte om de constructieve staat van de kunstwerken te beoordelen met als doel de levensduur mogelijk te verlengen.

Sinds de bouw van veel van deze kunstwerken zijn er nieuwe inzichten verkregen over mechanismes die kunnen leiden tot het falen van een kunstwerk. Een van deze mechanismes is degradatie ten gevolge van door chloriden geïnduceerde corrosie. Chloriden tasten de wapening aan, met als gevolg dat de capaciteit van de constructie afneemt. Dit wordt in de praktijk opgelost door grotere betondekkingen toe te passen. Hoewel dit een effectieve oplossing lijkt, ontbreekt het aan een methode waarin deze effectiviteit gekwantificeerd kan worden.

Onderzoeksvragen (WAT)

Hoe ziet een raamwerk voor het voorspellen van de technische restlevensduur van waterbouwkundige constructies in een maritiem milieu eruit? En hoe kunnen monitoring en inspecties bijdragen aan het verlengen van de verwachte restlevensduur?

Onderzoeksaanpak en -methode (HOE)
In deze studie combineren we bestaande door chloriden geïnduceerde corrosiemodellen met de theorie van constructieve betrouwbaarheid. Het raamwerk dat hieruit ontstaat, stelt ons in staat om de invloed van degradatie te relateren aan de prestatie van een constructie. Op basis van deze prestatie kan bepaald worden wat de verwachte restlevensduur is. Vervolgens passen we dit raamwerk toe op een tweetal hypothetische voorbeelden die typerend zijn voor een constructie gebouwd aan de Nederlandse kust. In deze voorbeelden wordt een betonnen balk gemodelleerd conform de vigerende rekenregels. Vervolgens worden dezelfde voorbeelden met het raamwerk doorgerekend om aan te tonen wat de verwachte levensduur is en hoe deze zich verhoudt tot de normen. Voorafgaand aan het onderzoek is een literatuurstudie uitgevoerd waarin de state-of-the-art van chloride-geïnduceerde corrosiemodellen in kaart is gebracht. Deze studie is uitgebreid met de kennis die TNO intern heeft.

Onderzoeksresultaten en synthese
Chloride geïnduceerde corrosie is gemodelleerd in twee fasen: de initiatiefase, waarin chloride-ionen migreren naar de wapening; en de propagatiefase, waarbij de vorming van corrosieproducten tot een afname van het wapeningsoppervlak leidt. Dit is een belangrijke parameter bij het bepalen van de capaciteit van een constructie. De capaciteit is voor twee faalmechanismes bepaald: voor het buigend moment en voor de dwarskracht. De capaciteit wordt in meerdere snedes van de constructie getoetst. Hierdoor kunnen ruimtelijke variaties in rekening gebracht worden, wat ons in staat stelt om een zo realistisch mogelijke inschatting te maken van de prestatie.
In de hypothetische voorbeelden is gevarieerd met de betondekking. In dit voorbeeld blijkt dat bij een dekking van 45 mm een verwachte levensduur van 160 jaar gevonden wordt. Bij een betondekking van 75 mm kon de verwachte levensduur niet bepaald worden omdat de simulatie na 200 jaar stopt.

Evaluatie en vooruitblik
Het chloride geïnduceerde corrosiemodel is succesvol geïntegreerd met de theorie van de constructieve betrouwbaarheid. Daarmee stelt het een asseteigenaar in staat om een voorspelling te doen van de verwachte restlevensduur van een constructie. Het raamwerk biedt tevens de flexibiliteit om resultaten uit monitoring en inspecties toe te voegen. Dit geeft de eigenaar de mogelijkheid om een onderhoudsstrategie te bepalen. Er zijn ook mogelijkheden om het raamwerk te verbeteren. Zo is in het raamwerk geen rekening gehouden met trends in belastingen. De prestatieberekening worden uitgebreid door een trend in de variabele belasting mee te nemen. Daarnaast kan het raamwerk niet gebruikt worden voor voorgespannen betonnen constructies.

TNO innovation for life

Chloride-induced corrosion

Remaining service life prediction of concrete structures in marine environments

TNO Public › TNO 2025 R10142
22 January 2025

Mobility & Built Environment
www.tno.nl
+31 88 866 20 00
info@tno.nl

TNO 2025 R10142 – 22 January 2025

Remaining service life prediction of concrete structures in marine environments

Chloride-induced corrosion

Author(s)	H.J.J. Weijs, G.A. Torres-Alves, H.G. Burggraaf, R.D.J.M. Steenbergen
Classification report	TNO Public
Number of pages	35 (excl. front and back cover)
Number of appendices	1
Project number	060.60155

Summary

As a result from the flooding of 1953, the Dutch government initiated the Delta Works project. The Delta works constitute of a series of hydraulic structures that mainly protect the country from flooding, particularly from sea. These structures should withstand the most severe conditions expected during their designed operational lifespan, approximately 100 years, with sufficient reliability. Currently, a full probabilistic life time assessment has not been performed on a hydraulic structure yet. Factors such as a changing climate exert adverse effects on the technical end of life. Conversely, new insights in material degradation provide possibilities to more accurately estimate the remaining service life. This report presents a reliability based framework to assess the remaining service life of a hydraulic structure in a marine environment. A structural reliability model is combined with a probabilistic corrosion-induced degradation model. The initiation model follows from the DuraCrete research and is extended with the DuMacon study, which zooms in on the Dutch coast. A propagation model is adpoted from literature. The structural capacity is determined through a combination of the FprEN 1992-1-1 (2021) and the fib Model Code 2020. This framework is then used to predict the remaining service life of a hydraulic structure with dimensions that are typical near the Dutch coastline. The framework accounts for temporal and spatial variations of input variables. The probability of failure is estimated using a Monte Carlo simulation that has been tested on a theoretical example with varying concrete covers (45 and 75 mm). The presented framework was successful in determining the expected annual conditional reliability index. The created framework allows to include additional information from e.g. inspections or measurements to update the reliability. The expected outcome is that by reducing the uncertainty, the reliability will increase. This will be investigated in future work.

Contents

Appendix

1 Introduction

1.1 The Dutch water engine

The Netherlands has been shaped by its close relationship with water. Its location along the North Sea coast and the confluence of two major rivers, the Meuse and the Rhine, has had a significant impact on the history and development of the country. However, this has presented unique challenges, making the country susceptible to floods.

In response, the Netherlands started the Delta Works project. This project focuses on the south-western region of the country and includes dikes, dams, storm surge barriers and other water regulatory objects to protect the country from flooding. Most of these structures serve multiple purposes, including flood protection, water regulation, and freshwater retention. Additionally, they facilitate the transportation of goods via rivers and canals, contributing to the country's economic output

Quantitative risk analysis
Hydraulic structures must meet defined performance requirements and demonstrate that they comply within these standards. A structure can fail to meet its performance requirements in multiple ways. A fault tree analysis is a common method used to examine these potential failure mechanisms. This approach deconstructs an undesired top (or main) event into progressively smaller events until only fundamental (also called basic) events remain. Each basic event is assigned a probability of occurrence. The connections between these basic events are determined through conditional or sequential logic. By considering each event, its probability of occurrence, and the logical interrelationships, fault tree analysis allows to calculate the probability of the undesired top (main) event. Consequently, the probability of failure of each identified failure mechanism (the undesired top/main event) can be determined.

1.2 Aging infrastructure

Every structure is designed to withstand the most severe conditions expected over its operational lifespan with a sufficiently high level of reliability. Typical hydraulic structures are constructed with a design technical lifespan of approximately 75-100 years. However, factors such as the rapidly changing climate and material degradation are increasingly affecting the remaining service life of these structures. Many of them are now well beyond halfway of their expected service life. Replacing these structures - especially the storm surge barriers - would incur billions of euros in costs. Additionally, the initiation, design, and construction of new structures would take a significant amount of time, including demolition of the existing structures. Therefore, exploring methods to assess and possibly extend the remaining service life of these structures could bring significant financial and social benefits.

Currently, the performance of these structures is typically assessed using fault tree analysis. An alternative methodology to estimate the probability of failure of structures under specific failure mechanisms is a time-dependent reliability assessment. This approach evaluates the probability of reaching a defined limit state and focuses on its evolution over time. A distinct advantage of this methodology over fault tree analysis lies in its ability to encompass temporal dependencies between variables of interest. This approach allows a more accurate estimation of the remaining service life of a structure.

1.3 Goal of this study

One of the failure mechanisms that might affect the capacity of hydraulic structures is associated with the corrosion of the reinforcement. This is particularly harsh in marine environments. Coastal exposure to saline conditions leads to durability challenges, including corrosion of the embedded reinforcing steel due to chloride ingress. This corrosion can eventually reduce the load-bearing capacity of the structure and ultimately lead to failure.

This report aims to combine existing chloride-induced corrosion degradation models with structural reliability theory, with a special focus on Dutch coastal environments. Limit states are defined to account for the effect of corrosion on the resistance. Corrosion models are examined in relation to these limit states. Where possible, variables in these models are stochastically quantified. The quantification is based on a literature review on the reliability-based estimation of concrete structures in marine environments, emphasizing chloride-induced corrosion, which can be read in a complementary report (TNO 2025 R10108). To demonstrate its practical application, the framework is applied to a theoretical example of a 10-meter simply supported beam. Two scenarios are investigated, with concrete covers of 45 mm and 75 mm, to show the influence of chloride-induced corrosion on the annual reliability of the beam. The application also considers the spatial variability of concrete properties.

The main goal of this report is to present a framework for assessing the structural performance and remaining service life of hydraulic structures — such as storm surge barriers — under Dutch coastal conditions. Additionally, a basis for conducting updated service life estimations based on new information is established. This information could follow from measurements or inspections.

1.4 Limitations

In this report existing chloride-induced corrosion degradations models are combined with the theory of structural reliability. This creates a framework where the remaining service life of a structure subjected to degradation can be estimated. This framework has limitations as well, which are mentioned below.

Corrosion induced degradation is a phenomenon that is not fully understood yet. The applicability of the degradation models used in this study is a point of discussion in the academic world. Especially in the latter stage, when corrosion products are formed, the suitability of the models is debatable. The first stage, where chloride ions migrate towards the rebar, is better understood.

The bond between the concrete and the rebar reduces as a result of corrosion. The underlying physics are not part of this study. Instead, a practical approach is adopted where a reduced bond factor is taken into account.

Corrosion products, which are being formed on the concrete-rebar interface, are expansive. This expansion induces additional stresses in the concrete, which can ultimately lead to the cracking and spalling of concrete. These effects are beyond the scope of this study. Other effects of corrosion, such as a reduced cross-sectional stiffness or the decrease in steel ductility are neglected as well.

The hydraulic structures within the scope of this study are typically prestressed. This is left outside the scope of this study, because there is insufficient confidence in the applicability of current models.

Finally, the presented limit state functions are related to the case study. This case study uses a simple element to showcase the applicability of the framework. For more complex elements, such as statically indeterminate structures, the limit state functions need to be derived such that they properly describe the failure domain.

1.5 Structure of the report

Chapters 2 and 3 establish the mathematical background needed to evaluate the reliability of structural elements. Specifically, Chapter 2 introduces key concepts and definitions from probability theory, while Chapter 3 presents the principles of structural reliability. Using this theoretical background, Chapter 4 presents a method for modeling chloride-induced corrosion. To illustrate the methodology, an example is presented in Chapter 5, where a simple structural component is simulated with dimensions and beam parameters chosen which are typical for Dutch coastal structures. Chapter 6 applies a probabilistic approach to assess the performance of the beam over time, including time-dependent factors such as degradation and also spatial dependencies for a comprehensive assessment. The results of this assessment and their interpretation for hydraulic structures near the Dutch coastline are presented in Chapter 7. Conclusions of this study and recommendations are summarized in Chapter 8.

2 Key concepts and definitions

2.1 Introduction

The goal of this report, as introduced in Chapter 1 is to combine chloride-induced corrosion models with structural reliability theory. Structural reliability encompasses concepts such as probability theory, and temporal and spatial dependencies. This allows to estimate the probability of failure of storm surge barriers under chloride-induced concrete corrosion.

This chapter aims to provide the theoretical basis for these methodologies so that they can be applied in the remaining chapters of this report. This chapter is by no means an exhaustive literature review of probability theory. It acts as an introduction to the concepts.

2.2 Random variables

A random variable, also known as a stochastic variable, is a variable whose exact value cannot be established. It can also be defined as a function that assigns values to the possible outcomes of an experiment. Random variables are used to quantify the results of random events and can take on many values, either discrete or continuous. More formally, a random variable X is a measurable function $X : \Omega \to E$ where Ω is the sample space of possible outcomes, and E is a measurable space. In other words, a random variable is a variable whose possible values are the numerical outcomes of a random phenomenon.

An important part of understanding and describing the behavior of a random phenomenon is the likelihood of such outcomes. In this way, probability distribution functions are introduced. For a continuous random variable X, the cumulative distribution function (cdf) is defined as the integral of its probability density function f_X. Figure 2.1 illustrates a general continuous probability density function and cumulative distribution function.

$$F_X(x) = P(x \leq x) = \int_{-\infty}^{x} f_X(x)dx \tag{2.1}$$

where $P(X \leq x)$ represents the probability that X takes on values less than or equal to x.

In real-life scenarios, analyzing a single random variable might not be sufficient to fully describe complex phenomena. In such cases, it is important to consider multiple random variables simultaneously and understand how they relate to each other. This relationship can be quantified by the concept of correlation, discussed in the next section.

2.3 Correlation

Correlation measures the strength and direction of the linear relationship between two random variables, indicating how one variable tends to increase or decrease in response to changes in

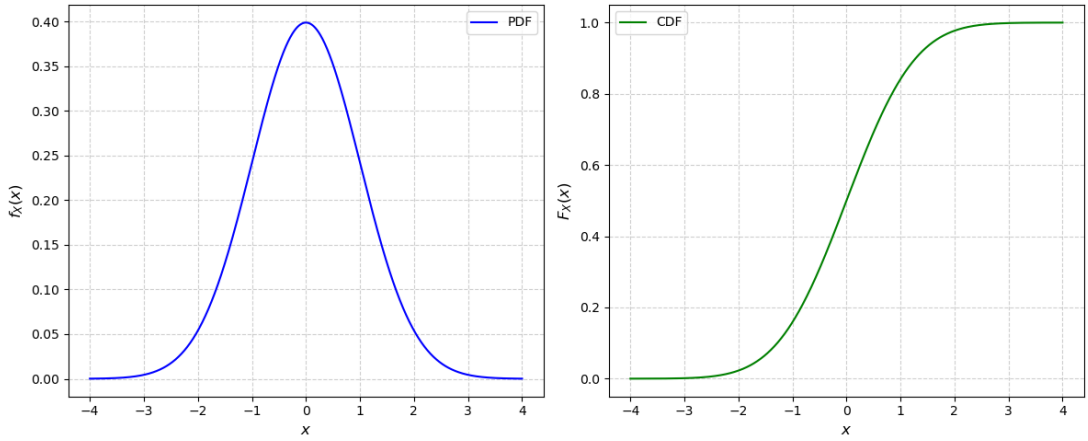

Figure 2.1: Probability (left) density function and cumulative (right) distribution function for a continuous variable.

the other in a consistent and straight-line manner. It helps to understand how the occurrence of one event might influence the other. There are several measures of the strength and direction of dependence between two random variables [1]. The most common are; i) Pearson product-moment correlation; ii) Kendall's tau; and iii) Spearman's rho.

2.4 Spatial variability

Spatial variability refers to the variation of a random property between different locations in the spatial domain. In many applications, the properties of interest (e.g., soil properties, material strength) are not uniform across the space, nor are they completely uncorrelated. Some form of correlation exists between two locations.

Spatial correlation describes the dependence of a variable between two different points in space. This dependence can be expressed in terms of a covariance function and the correlation length L, which represents the distance over which two variables show a strong spatial correlation. A high correlation length indicates that a variable is more likely to have similar properties when evaluated between two nearby points.

Spatial correlation can be described mathematically. The function that describes this is called a covariance function. A covariance function quantifies how a random variable at two different locations is related based on the distance between them. For two points in space of a studied random field X, $X(s_1)$ and $X(s_2)$, where s_1 and s_2 represent spatial coordinates, the covariance function is given by

$$\text{Cov}\left(X\left(s_1\right), X\left(s_2\right)\right) = \text{Cov}(d) = \sigma^2 \rho(d) \tag{2.2}$$

where σ^2 is the variance of the random variable X, $\rho(d)$ is the correlation function and $d = |s_2 - s_1|$ is the distance between the spatial coordinates s_2 and s_1. A correlation function describes how the correlation between values decays for increasing distances. Two models are the Exponential model and the Gaussian model. The Exponential model is defined as

$$\rho(d) = e^{-(d/L)} \tag{2.3}$$

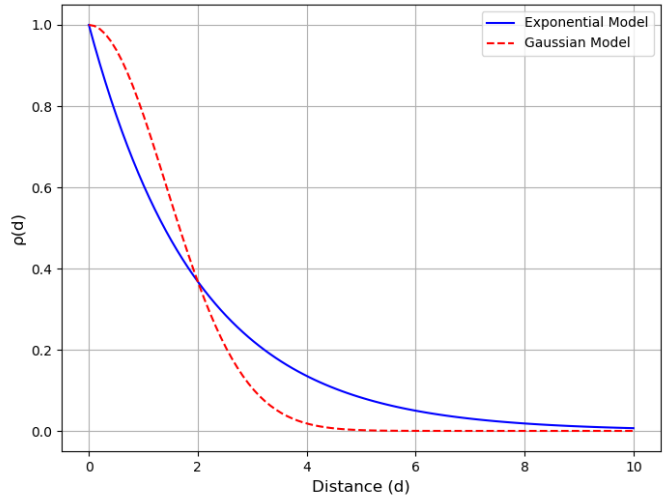

Figure 2.2: Exponential (blue) and Gaussian (red) correlation models.

where d is the distance between two points and L is the correlation length. The Gaussian model, also known as the Exponential-squared model, is

$$\rho(d) = e^{-(d/L)^2} \tag{2.4}$$

Compared to the Exponential model, the Gaussian model shows a stronger decay. This becomes more significant for larger distances. See figure 2.2 .

3 Structural reliability

3.1 Introduction to limit states

During its lifetime, a structural element must meet one or more functional requirements. To demonstrate its ability to meet these function(s), an elements' performance needs to be quantified and compared to regulations. A system's performance regarding to strength can be assessed using the following inequality:

$$R > S \tag{3.1}$$

where R is the resistance of the system and S is the solicitation (or load). If R and S are deterministic quantities, the safety of a system can easily be determined using Equation (3.1). However, in practice, both the load effects and the resistance are not considered deterministic quantities, but a function of multiple random variables. These random variables can be described by a distribution type and parameters. The result is that now the inequality in expression 3.1 can be expressed in terms of a probability of failure

$$P_f = P\left[R < S\right] \tag{3.2}$$

This problem can also be described by introducing a *limit state function*. The limit state describes the solution space in which the performance is sufficient to withstand its intended functional requirements. The limit state Z is determined as

$$Z = R - S \tag{3.3}$$

Failure occurs when $R < S$, or in other words, when $Z < 0$:

$$P_f = P\left[Z < 0\right] \tag{3.4}$$

3.2 General formulation for limit state design

A system can fail in multiple ways. This means that the solution space may contain multiple limit states. This is commonly denoted by a function that describes these different limit states

$$g\left(\mathbf{X}\right) = Z \tag{3.5}$$

where $\mathbf{X}$ is a vector containing all the variables that describe the limit state functions and $g\left(\mathbf{X}\right)$ is the limit state function (LSF). It is defined such that $g\left(\mathbf{X}\right) > 0$ describes the solution space in which the resistance is larger than the solicitation.

When $f_{\mathbf{x}}(\mathbf{x})$ describes the probability density function of the basic variables X_i, the failure probability is defined as:

$$P_f = \int_{g[\mathbf{x}]<0} f_{\mathbf{x}}(\mathbf{x})\, d\mathbf{x} \tag{3.6}$$

Reliability index β
The reliability index β measures the ability of a structure or structural element to meet the prescribed requirements during its intended design lifetime. It is related to the probability of failure through:

$$P_f = \Phi(-\beta) \tag{3.7}$$

where $\Phi(x)$ is the cumulative density function of the normal distribution. Building standards prescribe values of the target reliability β_t for a given return period. This target reliability corresponds to the required level of performance a structure must meet over that return period (e.g. EN 1990 (2019), NEN 8700 (2011) [2, 3]).

3.3 Time dependent reliability

Equation (3.6) returns the probability of failure which is valid at a certain reference period t_{ref}. This indicates that x describes the limit state function invariant of time (for a certain point in time). In practice, variables can show a trend with respect to time. For example, hydraulic loads could increase over time as a result of sea level rise. To include time effects in the limit state, eq. (3.6) can simply be extended by describing the limit state as a function of time:

$$P_f(t) = \int_{g[\mathbf{X}(t)]<0} f_{\mathbf{X}}(\mathbf{X}(\mathbf{t}))\, d\mathbf{X} \tag{3.8}$$

The result is that the probability of failure (or the reliability index) can be expressed a function of time. With this, it becomes possible to estimate the point in time at which a structure is expected to no longer fulfill its requirements (defining its end of service life). Figure 3.1 illustrates this.

Reaching the end of the service life time does not necessarily mean that the structure should be strengthened or renovated. It indicates that, given the current state of information, the reliability becomes smaller than the target reliability. It is therefore useful to update the information about the future behavior of the variables because that will lead to a more accurate life time prediction and may result in a higher reliability.

Once the service life associated with the target reliability is reached, a new assessment can be conducted to update the current estimate of the reliability. This assessment can be enhanced by updating the parameters of the variables through measurements and/or inspections. This is depicted in Figure 3.2 where, once the target reliability level is reached (at t_{ref1}), a new assessment is performed which shows that the actual reliability index is higher than what was initially forecast. This can be repeated multiple times. The end of life of a structure or a structural element is reached once, after having updated the relevant parameters, the estimated remaining service life is smaller than 1 year.

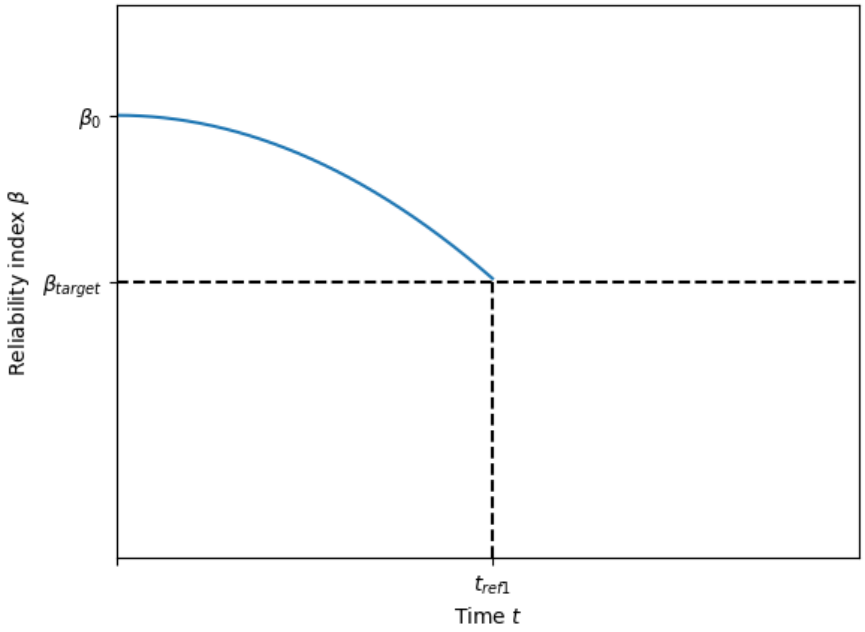

Figure 3.1: Definition of life time.

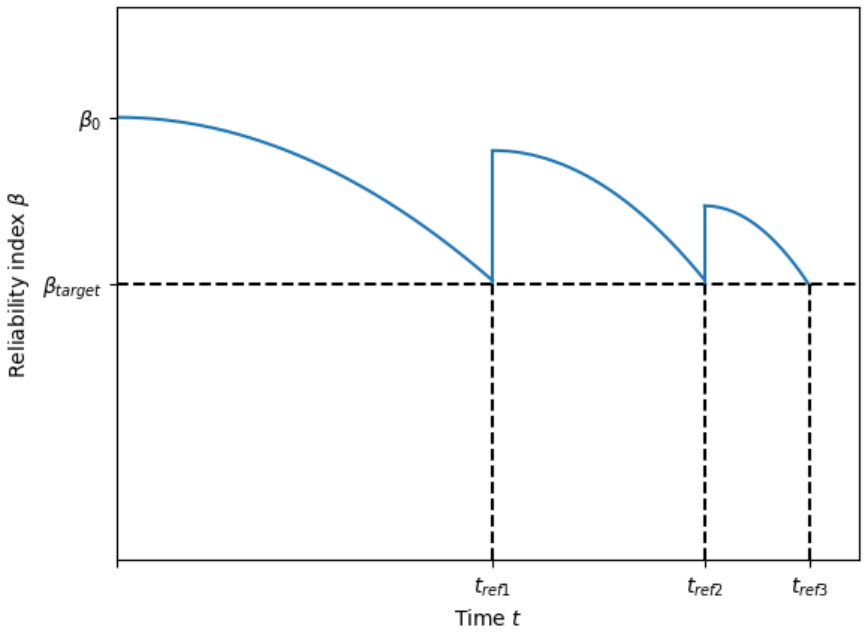

Figure 3.2: Life time extension through inspections.

4 Chloride-induced corrosion

4.1 General

Under normal conditions, concrete protects the embedded reinforcing steel against corrosion, which is attributed to a passive oxide film that forms on the surface of steel in a highly alkaline environment provided by the concrete pore solution. Two main causes can disrupt the protective properties of concrete: i) carbonation; or ii) penetration of chlorides [4]. This report focuses on chloride-induced corrosion as it is more relevant for coastal hydraulic structures.

Chloride ingress typically results from external sources, such as structures situated in maritime environments, the usage of deicing salts, or due to chloride-contaminated soils [5]. The penetration of chloride ions into concrete is a complex process described mainly by two transport mechanisms: ion diffusion and absorption. This process depends on several factors, including the properties of the concrete, the degree of concrete pore saturation, and the exposure conditions at the concrete surface. Many of these factors are influenced by time, spatial variations, and temperature[6].

A two-stage process

The service life of reinforced concrete structures, in the context of reinforcement corrosion, can be described in two stages [7, 8, 9]: i) the first stage, or initiation phase, is characterized by the reinforcement remaining passive. During this phase, phenomena such as chloride penetration into the concrete cover take place, potentially leading to the loss of passivity, ii) the second stage, also known as the propagation phase, begins when the steel becomes depassivated and continues until the effects of corrosion reach a level that is no longer acceptable. The propagation period starts when corrosion starts. In this stage, the structure deteriorates due to the reduction of steel cross-sectional area. Other effects of corrosion, for instance effects on the bond between concrete and steel, are not investigated in this research. A practical approach is applied by referring to building standards. The propagation stage lasts until an unacceptable degree of corrosion damage has occurred, impacting the load bearing capacity of the structure and/or its serviceability.

Most mathematical models that simulate chloride-induced corrosion focus on the initiation phase. In these models, the beginning of reinforced steel depassivation marks the end of the service life [10, 11, 12, 13]. However, according to [14], the safety of the structure is only diminished or impacted when there has been a loss of the reinforced steel cross-sectional area or loss of bond at the steel-concrete interface. Design strategy for service life modeling related to corrosion of reinforcement typically uses initiation phase models for the design of new structures and propagation stage models for the evaluation of structures already in service with depassivated reinforcement [15].

Section 4.2 presents a model to estimate the chloride content at a certain depth z (e.g., at the depth of the reinforcement) in the concrete. This represents the initiation period. Once the chloride content reaches as certain threshold value, the steel depassivates, and corrosion may occur. The model to describe this phenomenon is presented in section 4.3.

4.2 Chloride ingress model

Chloride ingress in concrete results from the complex interaction of different processes that after a certain time of exposure result in a chloride concentration profile [5]. The limit state function (LSF) is expressed as the difference between the critical (threshold) chloride concentration and the chloride concentration at the rebar surface at time t of the design working life

$$g(X,t) = C_{crit} - C(c,t) \tag{4.1}$$

where C_{crit} is the chloride content required to achieve depassivation of the reinforcement, $C(c,t)$ is the chloride content at the depth c and time t, c is the concrete cover, and t is the period of time under consideration. In the initiation phase, no loss of capacity is occurring, resulting in a time-invariant reinforcement area, i.e.: $A_s(t) = A_{s0}$.

Chloride ingress is modeled as a diffusion process using Fick's 2nd law of diffusion and the chloride content at depth z and time t can be calculated using [16]

$$C(z,t) = C_i + (C_s - C_i)\,\text{erfc}\left(\frac{z-\Delta z}{2\sqrt{D_a(t)\cdot t}}\right) \tag{4.2}$$

where $C(z,t)$ represents the chloride concentration at depth z after exposure time t, C_i is the initial chloride content present in the concrete matrix, C_s is the surface chloride content, erfc$(.)$ is the complementary error function, Δz is the depth of the concrete absorption zone and $D_a(t)$ is the time-dependent diffusion coefficient [16]. This model assumes that the surface chloride concentration C_s remains constant over time.

The reached (or apparent) diffusion coefficient $D_a(t)$ follows from

$$D_a(t) = D_{a,ref} \cdot \left(\frac{t}{t_{ref}}\right)^{-m} \tag{4.3}$$

where $D_{a,ref}$ is the diffusion coefficient at reference time t_{ref}, and m is the age factor [12]. It is assumed that the apparent diffusion coefficient remains constant over time t and changes only when the duration of the time period changes. In other words, it characterizes the average diffusivity over time period t. $D_{a,ref}$ is estimated as

$$D_{a,ref} = k_G \cdot D_{ref,0} \tag{4.4}$$

where $D_{ref,0}$ is the reference value determined in a chloride test at a short reference time and k_G is a coefficient for the characterization of the environmental and curing conditions. According to [17], different environmental coefficients apply for marine environments at the underwater, tidal, splash, and atmospheric zones. The values of the coefficients under these zones vary widely. Gehlen [18] suggests that concrete structures near the sea remain wet over time and that post-treatment or drying has little effect on chloride transport. The tidal and splash zones are most critical critical due to drying and wetting cycles. Thus, these areas are

investigated in this report. Another study has showed that this statement holds for structures near the Dutch coastline [19]. In this report, we follow this assumption. Gehlen [18] also suggests that for the same type of cement, only temperature affects chloride transport. The environmental and curing conditions can then be combined into one coefficient, k_G, defined as

$$k_G = \exp\left(b_e\left(\frac{1}{T_{ref}} - \frac{1}{T_e}\right)\right) \tag{4.5}$$

where b_e is a regression parameter, T_{ref} is a reference temperature, T_e represents the annual average ambient temperature and b_e is a regression parameter.

Once eq. (4.2) exceeds a threshold value C_{crit}, the initiation phase is completed and the propagation phase begins.

4.3 Propagation phase

Once the chloride content at the rebar has surpassed the chloride critical level, the propagation phase starts. During this period, corrosion products are created and a corrosion current is formed, which lead to a reduction in steel cross section. Under the assumption that the corrosion rate is a stationary process, the relationship between electrical current and the annual loss of rebar radius is [20]

$$\lambda \approx 0.0116 \cdot i_{corr} \tag{4.6}$$

where λ is the loss of the radius of the cross-section of the steel (for a rebar, in mm/year) and i_{corr} is the corrosion rate (in μA/cm^2). In [21] the right-hand side of the equation is multiplied by a factor R that includes the effect of localized pitting, which is characteristic for chloride-induced corrosion.

In this study, the model of [21] is chosen as it specifically refers to chloride-induced corrosion, but other models might have also been applicable. The corrosion rate is based on a study by[22], who exposed uncracked concrete specimen to salt spray conditions.

[21, 23] suggest to estimate the reduction in the reinforcement area using

$$A_s(t) = \frac{1}{4}\pi\left(D_0 - z\left(t\right)\right)^2 \cdot n_r \tag{4.7}$$

where $A_s(t)$ is the deteriorating reinforcement area, D_0 is the initial rebar diameter, $z(t)$ is the reduction in rebar diameter as a result of corrosion and n_r is the number of rebar. It is assumed that all n_r bars deteriorate in the same way. The equation to determine the deteriorating rebar diameter is given by [21]

$$D(t) = \begin{cases} D_i & \text{for } t \le t_i \\ D_i - 2\lambda\left(t - t_i\right) & \text{for } t_i \le t \le t_i + D_i/(2\lambda) \\ 0 & \text{for } t > t_i + D_i/(2\lambda) \end{cases} \tag{4.8}$$

where t_i is the time at which the initiation phase is completed.

4.4 Degradation-based structural performance

Concrete structures are typically reinforced to increase the capacity. Tensile stresses are resisted by the reinforcement and compressive stresses by the concrete. Degradation mechanisms, such as chloride-induced corrosion, compromise the capacity. Degradation results in a decreased rebar diameter, which compromises the tensile and therefore the structural capacity. This section shows how the bending moment capacity, M_R and the shear force capacity V_R are influenced by the reduction in rebar area.

The bending moment resistance $M_R(x,t)$ follows from concrete mechanics. A bi-linear stress-strain relationship is adopted for the concrete. $M_R(x,t)$ is described using

$$M_R(x,t) = A_s(t) f_y \left(d - \frac{7}{18} x_u\right) \tag{4.9}$$

where $A_s(t)$ is the deteriorating reinforcement surface (see section 4.3), f_y is the yield strength of the reinforcement, d is the effective depth of the cross section and x_u is the height of the concrete compressive zone (see Chapter 5).

The basis of the shear resistance $V_R(t)$ is found in FprEN 1992-1-1 (2021)[FprEN1992:2024] because this is widely supported. However, this model does not take into account the effects of corrosion. The fib Model Code 2020 [24] shares the latest insights on the modeling of concrete structures, including the effects of corrosion. Both the FprEN 1992-1-1 and the fib Model Code 2020 are strain-based approaches, which means that the shear resistance is a function of the longitudinal strain. The shear capacity equation used in FprEN 1992-1-1 is extended with the corrosion model from the fib Model Code. $V_R(x,t)$ is described using [25]

$$V_R(x,t) = \frac{1}{3} \frac{\sqrt{f_c} b\, d}{1 + 120 \frac{\epsilon(x,t)\ d}{16 + d_g}} \tag{4.10}$$

where $\epsilon(x,t)$ is the longitudinal strain at position x and time t at the control depth level ($= 0.6d$), d_g is the maximum aggregate size, f_c is the concrete compressive strength and b is the width of the beam. The longitudinal strain is estimated using [25]

$$\epsilon(x,t) = 0.41 \frac{M_E(x,t)}{z A_s E_s} \cdot \frac{A_s}{A_s(t) \cdot k_{bond}} \tag{4.11}$$

with $z = 0.9d$. The term[1] $A_s/(A_s(t) \cdot k_{bond})$ is the increase in longitudinal strain in the reinforcement due to corrosion. The strain increases because the bond between the concrete and the steel decreases. This part of the equation is adopted from the fib Model Code 2020, with $k_{bond} = 0.75$ (moderate corrosion).

[1] In the analyses performed in this report, A_s in the term $M_E(x,t)/(zA_sE_s)$ was accidentally replaced by $A_s(t)$. The result is that the increase in strain is overestimated by a term $A_s/A_s(t)$. This is a conservative approach, which means that the actual reliability indices presented in Chapter 7 are larger. Since we are dealing with a fictitious case in this report to demonstrate the reliability based framework, the numerical values are of less importance and are therefore left unchanged.

5 Typical cases

This chapter introduces two typical cases. These cases are artificially created. They are chosen such that they represent a range of structures with typical dimensioning found in concrete structures in a marine environment. The goal is to illustrate the calculation methodology and to show the influence of degradation on the annual reliability.

5.1 Beam dimensions and parameters

The typical case is represented by a simply supported beam made of reinforced concrete. The beam dimensions are illustrated in fig. 5.1. No shear reinforcement is present. It is subjected to a permanent load G_k, and a variable load Q_k. All parameters are presented in table 5.1.

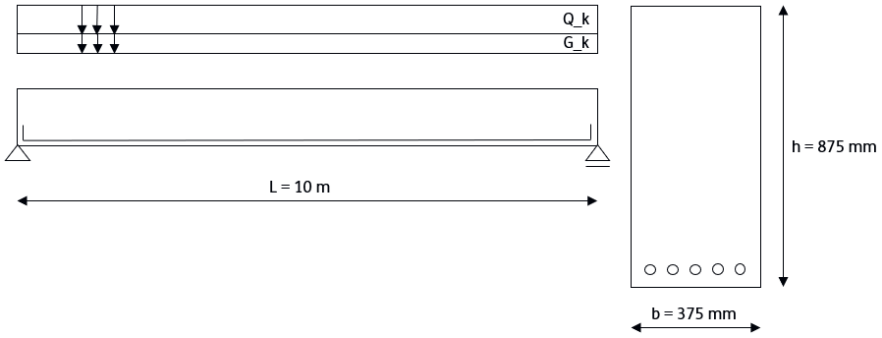

Figure 5.1: example case: beam dimensions.

Two distinctive cases are investigated: 1) one case where the concrete cover is equal to 45 mm. When following standard European design guidelines, this would be a normal value for the concrete cover; 2) one case where the concrete cover is equal to 75 mm. This is a value that is typically applied to Dutch hydraulic structures around the coastline, designed in the past by the Dutch Ministry of Transport (Rijkswaterstaat).

5.2 Solicitation functions

The beam is subjected to a permanent load G_k, and a variable load Q_k. Combined they lead to two types of external effects: a bending moment M_E and a shear force V_E. The total design load is

$$q_d = \gamma_G G_K + \gamma_Q Q_k \tag{5.1}$$

where γ_G, γ_Q are the partial factors for the permanent and variable load, respectively. Assuming the consequence class is CC2, the partial factors are $\gamma_G = 1.2$ and $\gamma_Q = 1.5$. The design load becomes $q_d = 42$ kN/m.

The external bending moment at any location x, $(0 < x < l)$, can be determined using

Table 5.1: Example: beam parameters.

Parameter	Variable	Value	Units	Note
Load parameters				
Permanent load	G_k	10	kN/m	-
Variable load	Q_k	20	kN/m	-
Concrete properties				
Beam length	l	10	m	-
Beam witdth	w	375	mm	-
Beam height	h	875	mm	-
Concrete cover (low)	c_{low}	45	mm	case 1
Concrete cover (high)	c_{high}	75	mm	case 2
Concrete compressive strength	f_{ck}	20	N/mm^2	C20/25
Maximum aggregate size	D_{max}	16	mm	-
Reinforcement properties				
Reinforcement strength	f_{yk}	220	N/mm^2	QR22
Youngs modulus	E_s	200000	N/mm^2	-
Number of rebar	n_{bar}	5	mm	-
Diameter of rebar	ϕ_{bar}	32	mm	-

$$M_{Ed}(x) = \frac{q_d x(l-x)}{2} \text{ for } 0 \leq x \leq l \tag{5.2}$$

and the external shear force through

$$V_{Ed}(x) = \begin{cases} q_d(0.5l - d) & \text{for } 0 \leq x \leq d \\ |q_d\left(\frac{1}{2}l - x\right)| & \text{for } d < x < l - d \\ q_d(0.5l - d) & \text{for } l - d \leq x \leq l \end{cases} \tag{5.3}$$

where $d = h - c - \phi_{bar}/2$ is the effective height of the concrete beam.

5.3 Capacity functions

The bending moment capacity of the beam is calculated using

$$M_{Rd} = A_s \frac{f_{yk}}{\gamma s}\left(d - \frac{7}{18}x_u\right) \tag{5.4}$$

where x_u is the height of the concrete compressive zone,

$$x_u = \frac{A_s \frac{f_{yk}}{\gamma_s}}{0.75 \frac{f_{ck}}{\gamma_c} b} \tag{5.5}$$

where $\gamma_s = 1.15$ is the partial factor which covers the uncertainties related to reinforcement steel and $\gamma_c = 1.5$ is the partial factor which covers the uncertainties related to concrete.

The design shear capacity is calculated using prEN 1992-1-1 (2021) eq. (I.7) [26]

$$V_{Rd,c} = 0.33 \frac{\gamma_{def}^{2/3}}{\gamma_V^2} \frac{\sqrt{f_{ck}}\, b\, d}{1 + 24\gamma_{def}\epsilon_V \frac{d}{d_{dg}}} \tag{5.6}$$

where $\gamma_V = 1.4$ is the partial factor that covers the uncertainties related to shear calculations, $\gamma_{def} = 1.33$ is the partial factor which covers the uncertainties related to the deformation calculations, ϵ_V is the strain in the longitudinal reinforcement and $d_{dg} = 16 + D_{max} = 32$ mm. The strain in the longitudinal reinforcement follows from

$$\epsilon_V = \frac{M_{Ed}}{zE_sA_s} \tag{5.7}$$

with $z = 0.9d$.

5.4 Design verification

Design verification is done through a level I reliability method. This is a semi-probabilistic method. Variables that are normally characterized by a distribution are represented by a characteristic value. The limit state evaluations are enhanced by partial factors. This results in a unity check (load over resistance ratio), which implies safe design when it is smaller than 1, and unsafe design when it is larger than 1. This is done for both the bending moment capacity and the shear capacity.

The unity check with respect to the bending moment is equal to the ratio between M_{Ed} (see eq. (5.2)) and M_{Rd} (see eq. (5.4)). In this case, the highest unity check is found at $x = l/2$, which yields:

$$uc_M = \frac{M_{Ed}}{M_{Rd}} = \begin{cases} \frac{525}{565} = 0.93 & \text{for } c = 45 \text{ mm} \\ \frac{525}{542} = 0.97 & \text{for } c = 75 \text{ mm} \end{cases} \tag{5.8}$$

The unity check with respect to the shear is equal to the ratio between V_{Ed} (see eq. (5.3)) and V_{Rd} (see eq. (5.6)). In this case, the largest unity check is found at $x = d$, which yields:

$$uc_V = \frac{V_{Ed}}{V_{Rd}} = \begin{cases} \frac{176}{206} = 0.85 & \text{for } c = 45 \text{ mm} \\ \frac{177}{199} = 0.89 & \text{for } c = 75 \text{ mm} \end{cases} \tag{5.9}$$

The unity checks indicate a well designed beam. The next chapter will look at the same example, but from a probabilistic point of view.

6 Time dependent reliability assessment

6.1 Limit state function

This section presents the limit state function of the beam. The limit state function describes the solution space in which the performance is sufficient enough to withstand its intended functional requirements. It is defined as

$$Z(t) = R(t) - S(t) \tag{6.1}$$

Where R and S are the resistance and solicitation functions, respectively (see also Chapter 3). Chapter 4 explained that corrosion is a two-step progress consisting of: 1) an initiation phase where chloride ions migrate towards the rebar but there is no loss of capacity yet; and 2) a propagation phase, in which the capacity is reduced as a result of a loss of reinforcement area. Because the initiation phase does not directly influence the capacity functions, this chapter does not describe this process. More information on the two phases can be found in Chapter 4.

6.1.1 Solicitation function

This section presents the equations that probabilistically describe the solicitation function. The equations presented in Chapter 5 implicitly took uncertainties into account by applying partial factors to characteristic values. In a probabilistic assessment these variables are described by a distribution type and parameters. The distribution type and parameters of all variables are presented in section 6.3.

The total load $q(t)$ on the system is the sum of the (time invariant) permanent load G and the variable load $Q(t)$:

$$q(t) = G + Q(t) \tag{6.2}$$

G and $Q(t)$ are completely described with a distribution type and parameters. It is assumed that the permanent load does not change with respect to time. The variable load can alter from year to year. Both loads are assumed to be fully spatially correlated.

The solicitation function $S(x,t)$ becomes

$$S(x,t) = \begin{bmatrix} S_1(x,t) \\ S_2(x,t) \end{bmatrix} = \begin{bmatrix} M_E(x,t) \\ V_E(x,t) \end{bmatrix} \tag{6.3}$$

where

$$M_E(x,t) = \frac{q(t)x(l-x)}{2} \quad \text{for } 0 \leq x \leq l \tag{6.4}$$

and

$$V_E(x,t) = \begin{cases} q(t)(0.5l-d) & \text{for } 0 \leq x \leq d \\ |q(t)\left(\frac{1}{2}l - x\right)| & \text{for } d < x < l-d \\ q(t)(0.5l-d) & \text{for } l-d \leq x \leq l \end{cases} \tag{6.5}$$

6.1.2 Resistance function

The resistance function $R(x,t)$ is:

$$R(x,t) = \begin{bmatrix} R_1(x,t) \\ R_2(x,t) \end{bmatrix} = \begin{bmatrix} M_R(x,t) \\ V_R(x,t) \end{bmatrix} \tag{6.6}$$

$M_R(x,t)$ is described using the following equation:

$$M_R(x,t) = A_s(t) f_y \left(d - \frac{7}{18} x_u\right) \tag{6.7}$$

where $A_s(t)$ is the deteriorating reinforcement surface (see section 4.3), f_y is the yield strength of the reinforcement, d is the concrete effective depth and x_u is the height of the concrete compressive zone.

$V_R(x,t)$ is described using [25]

$$V_R(x,t) = \frac{1}{3} \frac{\sqrt{f_c} b\, d}{1 + 120 \frac{\epsilon(t)\, d}{16 + d_g}} \tag{6.8}$$

where $\epsilon(t)$ is the longitudinal strain at the control depth level ($= 0.6d$), d_g is the maximum aggregate size, f_c is the concrete compressive strength and b is the width of the beam. The longitudinal strain is estimated using [25]

$$\epsilon(x,t) = 0.41 \frac{M_E(x,t)}{z A_s(t) E_s} \tag{6.9}$$

with $z = 0.9d$.

6.2 Method to assess the structural reliability

The structural reliability is assessed using the Monte Carlo method. Monte Carlo is categorized as a level III reliability method, that allows a more accurate estimation of the probability of failure, in contrast to approximation-based or semi-probabilistic methods.

Monte Carlo simulations rely on repeated random sampling to model a range of realistic scenarios. Each simulation generates a unique set of input samples, which leads to a unique output. In this case, the output for each simulation is the year at which the beam fails, if failure occurs.

Failure of the beam is expressed as a series system with two components: bending failure and shear failure. If one component fails, the beam fails. The mechanisms are evaluated every 0.5 m. The total length of the beam is 10 m, resulting in 21 sections, with 2 limit state functions being evaluated per time step, for each beam.

Conditional failure rates

The failure probabilities are derived from the output of the simulations. This report presents conditional failure probabilities, meaning that only structures that have survived up to a given time are considered in the calculation. The conditional failure probability at year i is defined as:

$$P_f(t = i) = \frac{n_{f,i}}{n_{s,i-1}} \tag{6.10}$$

where $n_{f,i}$ is the number of simulations that result in failure in year i, and $n_{s,i-1}$ is the number of simulations that survived the year prior. The relation between the probability of failure and reliability is presented in eq. (3.7).

6.3 Stochastic quantification of variables

Stochastic quantification is the process of using probabilistic methods to model and analyze uncertainties in systems with inherent randomness. Key variables, such as loads or material properties, are treated as random variables, and their uncertainties are represented by probability distributions. Table 6.1 presents the stochastic quantification of the variables that collectively define the entire system and were used as inputs in modeling chloride-induced corrosion in the academic example of Chapter 5. These parameters are essential to perform the reliability assessment, as described in the previous section.

Table 6.1: Stochastic quantification of variables.

Parameter	Symbol	Distr. type[1]	μ	CoV	Units	Mult. factor	Correlation length (m)	Covariance model	Source
Load parameters									
Permanent load	G	N	10	0.1	kN/m	1	-	-	[2]
Annual maximum variable load	Q	Gum	14.40	0.15	kN/m	1	-	-	[3]
Beam parameters									
Length	l	D	10	-	m	1	-	-	-
Initial rebar area	A_{s0}	N	4021	0.02	mm^2	1	-	-	[6]
Yield strength of steel	f_y	LN	280	0.11	N/mm^2	1	-	-	[6]
Concrete cover high	c_{high}	D	75	-	mm	1	-	-	-
Concrete cover low	c_{low}	D	45	-	mm	1	-	-	-
Concrete compressive strength	f_c	LN	28	0.06	N/mm^2	1	2	Gaussian	[6, 27]
Concrete beam width	b	D	375	-	mm	1	-	-	-
Youngs modulus of steel	E_s	D	200000	-	N/mm^2	1	-	-	[6, 28]
Bond factor high	$k_{bond,high}$	D	1	-	-	1	-	-	[24]
Bond factor low	$k_{bond,low}$	D	0.75	-	-	1	-	-	[24]
Granulate diameter	d_g	D	16	-	mm	1	-	-	[29]
Bar diameter	ϕ_{bar}	D	[4]	-	mm	1	-	-	
Number of rebar	n_r	D	5	-	-	1	-	-	
Chloride ingress parameters									
Surface chloride content	C_s	N	2.9	0.28	w.t.-%/b	1	2	Exponential	[19, 30]
Critical chloride content	C_{crit}	D	0.5	-	wt.-%/b	1	-	-	[19]
Initial chloride content	C_i	D	0.01	-	wt.-%/b	1	-	-	[19]
Concrete absorbtion zone	Δz	Beta[2]	2.10	9.56	mm	50	-	-	[16][5]
Reference chloride diffusion coefficient	$D_{ref,0}$	D	8.83E-05	-	m^2/year	1	-	-	[31]
Age factor	m	Beta[2]	23.97	25.97	-	1	-	-	[19]
Curing coefficient	k_G	N	0.56	0.08	-	1	2	Exponential	[19, 27][6]
Concrete degradation parameters									
Corrosion Rate	i_{corr}	N	1.0	0.2	$\mu A/cm^2$	1	-	-	[21]
Pitting factor	R	N	3.0	0.11	-	1	-	-	[21]

1: Distribution abbreviations are: D = deterministic; N = normal; LN = lognormal; Gum = Gumbel; Beta = Beta.
2: For the Beta distribution, the presented parameters are the α and β parameter instead of the mean and CoV.

Note 2
A permanent load is always present on a structure. Therefore they can be estimated quite accurately. These types of loads can be described by a normal distribution [32]. Its characteristic value is equal to its expected value. In the typical case the characteristic value for the permanent load, G_k, is taken equal to 10 kN/m. Therefore, the expected value of G is 10 kN/m. A coefficient of variation of 10% is assumed. No spatial correlation is considered:

$$G \sim \mathcal{N}(10,\, 1^2)\,.$$

Note 3
In the typical case the characteristic value for the variable load, Q_k is taken equal to 20 kN/m. This value presents a maximum value in a certain return period. It is assumed that this value belongs to a return period of 50 years, which means that the yearly exceedance probability is $\frac{1}{50}$. Furthermore it is assumed that the parameter can be described by a Gumbel distribution. The underlying equation to solve becomes:

$$P\left(Q > 20\right) = \frac{1}{50} \tag{6.11}$$

where

$$Q = F\left(x; \mu, \beta\right) = e^{-e^{-(x-\mu)/\beta}} \tag{6.12}$$

Assuming a coefficient of variation of 15%, eq. (6.12) can be solved for its location μ and scale β parameters, respectively. The result becomes

$$Q \sim \mathcal{G}(13.43,\, 1.68)\,.$$

Note 4
The bar diameter is calculated based on the sampled reinforcement area A_{s0}:

$$\phi = \sqrt{\frac{4A_{s0}}{\pi n_r}} \tag{6.13}$$

Note 5
[16] proposes a Beta distributed parameter on the interval [0, 50] with a mean value of 9 mm and a coefficient of variation of 0.6. Assuming the following parameters for a standard Beta distribution

$$\Delta z \sim \beta(2.098,\, 9.557)\,.$$

yields the following expected value and standard deviation:

$$E[\Delta z] = \frac{\alpha}{\alpha + \beta} = 0.18 \tag{6.14}$$

$$Var(\Delta z) = \left(\frac{\alpha\beta}{(\alpha+\beta)^2 \cdot (\alpha+\beta+1)} \right)^2 = 0.0117 \tag{6.15}$$

Multiplied by its interval, this results in $E[\Delta z]$ = 9 and a coefficient of variation of 0.6.

Note 6
In [27] a squared exponential model is assumed to describe the spatial variation in the chloride diffusion coefficient D_a. In the model that is used in this report, the diffusion coefficient is not described by a variable and therefore a spatial correlation model can not be assigned to it. The curing coefficient k_G, however, is sampled. Because D_a is described by a function that linearly depends on k_G, the variability is assigned to this variable, which ensures that D_a has the intended spatial variation.

6.4 Numerical Implementation

The steps to determine the year of failure and the corresponding failure mechanism are presented in the pseudo code below. The code is written in Python version 3.11.

```
FOR simulation in total number of simulations:

    beam_parameters = empty list
    section_results = empty list
    beam_results = empty list

    FOR variable in list of variables:

        ADD variable name to beam_parameters

        IF deterministic:
            FILL beam with deterministic values for all cross sections
        ELSE:
            IF correlation_length == 0:
                SAMPLE values for each cross section
            ELSE:
                GET uncorrelated samples
                CALCULATE covariance matrix
                DECOMPOSE correlation matrix (Cholesky)
                SAMPLE correlated values and assign to each cross section

    FOR each cross section in beam:

        CALCULATE external effects for each year:
            bending moment
            shear force

        INITIALIZE chloride migration and calculate concentrations

        IF corrosion_concentration > critical_value:
            CALCULATE corrosion degradation
            UPDATE capacity reductions (bending, shear)
```

```
        CALCULATE limit state functions (bending, shear)

        DETERMINE failure year and failure mode (bending, shear)

        IF no failure:
            failure_time = infinity

        ADD section results to section_results list

    DETERMINE beam failure time, mode, and location from section results:

        FOR each cross section in beam:
            IF cross section failure time < beam failure time:
                UPDATE beam failure time, mode, location

    ADD beam failure results (time, mode, location) to beam_results

    # Calculate the conditional probability of failure

    SET failed_simulations = 0 (initialize)
    SET surviving_simulations = total number of simulations
        - failed_simulations
    SORT beam_results

    FOR each year:

        GET number of failed simulations from beam results
        CALCULATE conditional probability of failure
        UPDATE failed_simulations
        UPDATE surviving_simulations
```

7 Results

This section presents the results of a theoretical example that illustrates the time-dependent reliability assessment of a concrete beam over 200 years. The methodology combines chloride-induced degradation models for both the initiation and propagation phases with structural reliability theory. Key factors such as the spatial variation of concrete compressive strength, surface chloride content, and curing coefficient are incorporated. The input parameters, including distributions and values for loads, beam properties, chloride ingress, and concrete degradation parameters, are detailed in Table 6.1.

It is important to note that this example is based on a simplified, theoretical model. In real-world applications, the specifics of the structure — such as whether it is statically determinate or indeterminate — must be considered. For example, for statically indeterminate structures, failure at a single location may not lead to overall structural failure, and the failure probability function may become more complex, depending on the context of the structure being analyzed.

7.1 Conditional reliability as a function of time

The beam from the example in Chapter 5 is discretized into 0.5 m sections for a detailed analysis. Each cross-section is evaluated yearly for bending moments and shear forces. The progression of corrosion is incorporated by assessing chloride-induced degradation over time. As described in Chapter 4, if the chloride concentration exceeds a critical threshold, the propagation of corrosion occurs in the beam's reinforcement. This leads to reductions in the beam's capacity. The corresponding limit state functions for bending and shear are then evaluated to estimate each cross-section's failure time and mode.

The beam's failure characteristics, such as failure time, mode, and location, are determined by identifying the earliest failure among its cross-sections. Then the conditional probability of failure of the beam over time is computed by iterating through several years, updating the counts of failed and surviving simulations, and deriving annual failure probabilities based on the sorted results. The conditional probability refers to the probability of failure given that no failures were registered in the previous years.

The reliability assessment was conducted for two cases with different concrete cover values: 45 mm and 75 mm, following the methodology outlined previously. Figure 7.1 shows the evolution of the annual reliability index, beta (β) [7], over time. The first case ($c = 45$ mm), represents the final design of a beam based on European design codes. The second case ($c = 75$ mm) corresponds to a scenario typically found in structures near the Dutch coastline.

Both cases were evaluated using 200 million simulations. To achieve fully converged results, it is required to have a higher number of simulations, around one to two orders of magnitude larger. This becomes more evident for larger reliability indexes ($\beta > 4$), where the insufficient number of simulations results in a more jagged curve. This was not feasible due to time constraints. Nevertheless, the results are sufficient to show the time dependence and to predict the remaining technical service life.

[7] The reliability index reflects the probability of failure, with higher values of β indicating lower failure probabilities.

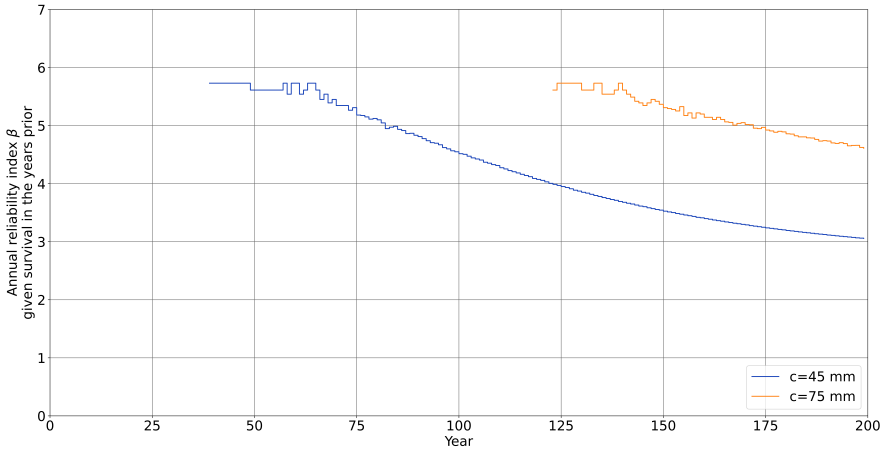

Figure 7.1: Conditional reliability level as a function of time for a concrete cover of 45 mm and 75 mm mm.

NEN 8700 (2011) [3] provides performance requirements for existing structures. for a structure with consequence class CC2, the minimum value of the reliability index $\beta = 2.5$, with a reference period of 15 years. In [33] this is translated to a reference period of 1 year: they determined that the minimum annual reliability index is $\beta = 3.4$. As shown in Fig. 7.1 , the reliability level of the beam with a concrete cover of $c = 45$ mm drops below this threshold after approximately 160 years. The reliability index of the beam with a concrete cover of $c = 75$ mm remains above the threshold of $\beta = 3.4$ even after 200 years, ensuring compliance with the requirements for existing structures.

Figure 7.2 shows the distribution of failures over time. Notice the increasing trend in failure occurrence as the years progress. This is expected due to structural aging and the progression of corrosion would lead to more frequent failures over time. Initially, failures occur at a slow rate. It can be seen that up to the year 100 failures are rare. However, beyond that point that rate of failures accelerates significantly. The figure extends to 200 years because a threshold was established, as failures beyond that timeline are not of relevance given that the intended lifetime of the structure is much shorter. In this way, it is ensured that the focus remains on the most critical and realistic period of the structure's performance. The figure also highlights the influence of the concrete cover depth on the observed number of failed simulations. The simulation with a concrete cover of $c = 75$ mm barely shows any failures compared to the simulations where the cover was 45 mm.

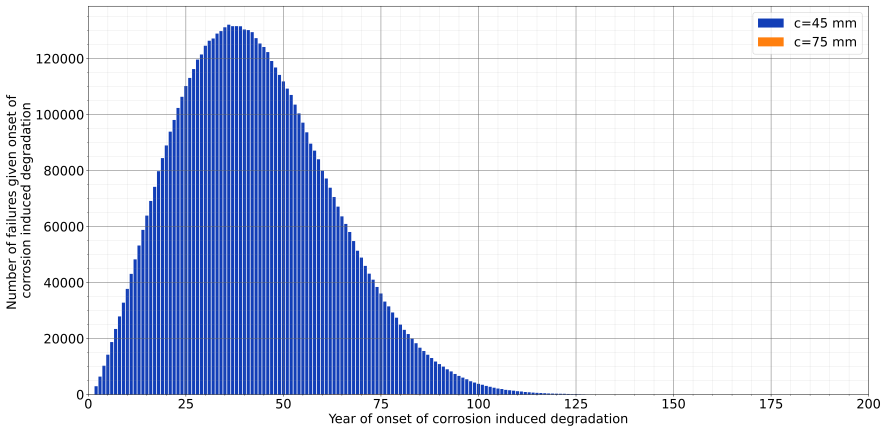

Figure 7.2: Distribution of number of failures over time for a beam with a concrete cover of $c = 45$mm and $c = 75$ mm.

It is also important to relate the time at which the propagation of corrosion starts and the time at which structural failure would occur. Figure 7.3 shows the distribution of the number of failures given that corrosion propagation started on a particular year. In other words, the x-axis describes the year on which the propagation started and the y-axis describes the number of failures in the experiment that were found under those conditions. Again, the beams with a concrete cover of 75 mm contribute insignificantly to the failure probability compared to the beams with a concrete cover of 45 mm.

The results for a concrete cover of c = 75 mm are very limited. The high annual reliability index indicates that corrosion-initiated failures are expected to be very limited. Figures 7.2 and 7.3 verify that the number of failed simulations is small - especially compared to the case where the cover is c = 45 mm.

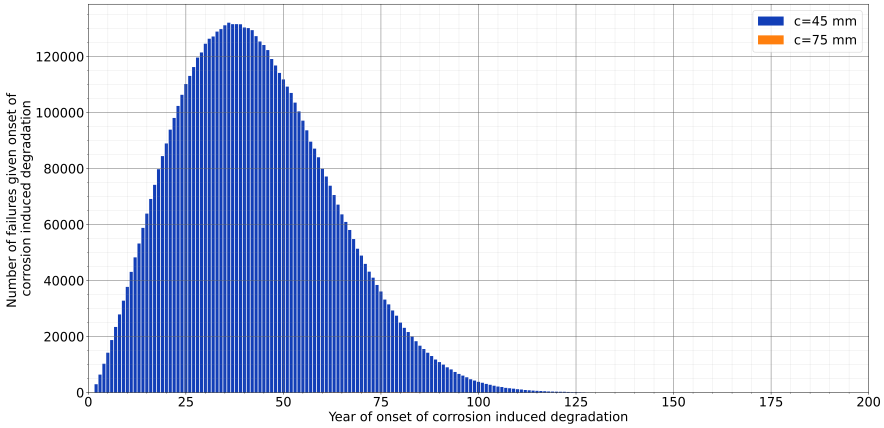

Figure 7.3: Distribution of the number of failures conditioned on the year when onset of corrosion occurs ($c = 45$mm and $c = 75$ mm).

The distribution peaks around year 50 ($c = 45$ mm), suggesting that corrosion propagation may lead to failure within this time frame. The tail of the distribution indicates that failures become less frequent the longer it takes for propagation to start. Thus, the further this propagation of corrosion is delayed, the fewer failures are expected within 200 years. Conversely, the rise in failures during the early years indicates that once corrosion propagation starts, it increases the likelihood of structural failure. From the figure, we can derive a ”critical” period between years 20-75, where structures are more susceptible to failure due to corrosion. This provides insights into maintenance schedules. For example, a best strategy could be to perform inspections during these years.

7.2 Measures to extend the remaining service life

As discussed in the previous section, the annual reliability of a beam with a concrete cover of $c = 45$ mm drops below the target value of 3.4 recommended by the NEN 8700 after 160 years. In contrast, for a beam with a concrete cover of $c = 75$ mm, the reliability index remains above this threshold throughout the 200-year time frame under consideration.

Several types of monitoring or inspection can be implemented in the developed Monte Carlo-based failure rate method. Such information can lead to an update of the calculated failure probability in a certain year of a predicted (remaining) service lifetime. Among these are visual inspections and additional chloride profile measurements. These actions are critical in reducing uncertainty in key variables (Chapter 6). Addressing these uncertainties improves the prediction of the conditional reliability index, as detailed in Chapter 3.

Chloride profile measurements refine parameter estimates by reducing the variation in model inputs. Additionally, condition monitoring allows a dynamic update of reliability assessments, ensuring that the interventions are based on current data. By reducing uncertainty, a more accurate remaining service life can be predicted. However, further studies are recommended to quantify the exact impact of different intervention strategies.

8 Conclusions and recommendations

8.1 Conclusions

This report presented a method to combine chloride-induced corrosion models with structural reliability theory to estimate the remaining service life of concrete structures, specifically near the Dutch coastal area. The methodology includes the two phases of chloride-induced degradation: i) phase one, where chloride ions migrate towards the rebar (modeled using Fick's 2nd law of diffusion). During this phase, degradation has not yet started, and ii) phase two, where corrosion reduces the diameter of the rebar leading to a loss of structural capacity and an increased likelihood of failure.

Two typical examples were used to show the influence of degradation on the annual reliability of a concrete beam, taking into account spatial variability in properties such as compressive strength, surface chloride content, and curing coefficients. A Monte Carlo simulation approach was employed to evaluate the beam's reliability over 200 years.

Two concrete cover depths were assessed: i) 45 mm, representative of typical European designs, and ii) 75 mm, commonly found in structures designed by Rijkswaterstaat near the Dutch coastline. The method is set up such that the structure-specific model data and additional information from monitoring or measurements can be used as input for the methodology presented in this document. This leads to an updated and more certain remaining service life estimation. This way, the reliability-based tool can greatly help asset owners estimate the remaining service life. It also allows the owner to continuously update this estimation, based on new information from measurements or monitoring, which contain key information to estimate the remaining service life of structures optimally.

8.2 Limitations and recommendations for future work

The chloride ingress and corrosion propagation models used in this study rely on simplified assumptions, including constant environmental conditions and uniform material properties. These assumptions may not fully capture real-world factors such as fluctuating chloride exposure, localized degradation, or the presence of cracks, damage, or repairs in the concrete. The analysis focuses on the reduction of rebar cross-sectional area but does not provide a solution for prestressed concrete. Thus, the findings are primarily valid for non-cracked, simply reinforced concrete conditions.

Nevertheless, the proposed framework is a valuable tool for understanding and modeling chloride-induced corrosion in reinforced concrete structures. It is important to note that this report presents a theoretical example, and the limit state functions and the input variables used (Table 6.1) may vary depending on the specific structure and its location. Future work should focus on extending the application of this methodology to real-world structures by integrating data from inspections and field measurements, such as chloride profiles,

environmental conditions, and load histories, to validate and refine the input variables and methodology. Incorporating temporal variations in environmental conditions, such as fluctuating water levels, would improve the accuracy of simulations. Moreover, expanding the scope to include cracked concrete conditions would significantly enhance the applicability of the framework. Addressing these limitations will enhance the framework and provide deeper insights into the durability and maintenance needs of coastal hydraulic structures.

References

[1] Claudia Czado. “Analyzing dependent data with vine copulas”. In: *Lecture Notes in Statistics, Springer* 222 (2019).

[2] Nederlands Normalisatie-instituut (NEN). *National Annex to NEN-EN 1990+A1:2006+A1:2006/C2:2019 Erocode: Basis of structural design*. 2019.

[3] Nederlands Normalisatie-instituut (NEN). *NEN 8700: Beoordeling van de constructieve veiligheid van een bestaand bouwwerk bij verbouw en afkeuren – Grondslagen*. 2011.

[4] J. Rodríguez, C. Andrade, and G. Somerville. “Manual for assessing corrosion-affected concrete structures”. In: *Geocisa and Torroja Institute, EC Innivation Programme, IN30902I* (2002).

[5] DuraCrete. “Modelling of degradation, DuraCrete–Probabilistic performance-based durability design of concrete structures”. In: *EU-BriteEuRam III, Contract BRPR-CT95-0132, Project BE95-1347/R4-5* (1998), p. 174.

[6] JCSS. “Probabilistic model code: Joint committee on structural safety”. In: *JCSS, Japan* (2001).

[7] Kyösti Tuutti. “Corrosion of steel in concrete”. English. Defence details Date: 1982-10-21 Time: 09:00 Place: KTH, Kungliga Tekniska Högskolan i Stockholm External reviewer(s) Name: Schiessl, Peter Title: [unknown] Affiliation: IBAC, Aachen —. Doctoral Thesis (monograph). Division of Building Materials, 1982.

[8] Zdeněk P Bažant. “Physical model for steel corrosion in concrete sea structures—Application”. In: *Journal of the structural division* 105.6 (1979), pp. 1155–1166. ISSN: 0044-8001.

[9] Luca Bertolini et al. *Corrosion of steel in concrete: prevention, diagnosis, repair*. John Wiley & Sons, 2013. ISBN: 3527651713.

[10] R.D. Browne. “Design prediction of the life for reinforced concrete in marine and other chloride environments”. In: *Durability of building materials* 1 (1982), pp. 113–125.

[11] Miki Funahashi. “Predicting corrosion-free service life of a concrete structure”. In: *ACI Mater. J* 87 (1990), p. M62.

[12] Magne Maage, Steinar Helland, and Jan Erik Carlsen. “Practical non-steady state chloride transport as a part of a model for predicting the initiation period”. In: *Proceedings of the 1st International RILEM Workshop*. 1995, pp. 398–406.

[13] L. Tang and L.O. Nilsson. “10 Service Life Prediction for Concrete Structures under Seawater by a Numerical Approach”. In: *Durability of Building Materials & Components 7 vol. 1* (2018), p. 97. ISSN: 1136746617.

[14] Rasheeduzzafar, S.S. Al-Saadoun, and A.S. Al-Gahtani. “Corrosion cracking in relation to bar diameter, cover, and concrete quality”. In: *Journal of Materials in Civil Engineering* 4.4 (1992), pp. 327–342. ISSN: 0899-1561.

[15] Beatriz Martın-Pérez. “Service life modelling of RC higway structures exposed to chlorides”. Thesis. Civil Engineering, 1999.

[16] JCSS. *Probabilistic Model Code - Part 2: Load Models*. 2020.

[17] J. Visser et al. *Statistical quantification of the variables in the limit state functions: DuraCrete, probabilistic performance based durability design of concrete structures*. Gouda: CUR, 2000. ISBN: 9037603742.

[18] Chr Gehlen. “Probabilistische Lebensdauerbemessung von Stahlbetonbauwerken. Deutscher Ausschuss für Stahlbeton, Heft 510”. In: *Beuth, Berlin* (2000).

[19] R.B. Polder and M.R. de Rooij. *Duurzaamheid Mariene Constructies (DuMaCon)*. Report 2004-CI-R0047-8. TNO, Sept. 2004.

[20] S. Lay, P. Schiessl, and J. Cairns. *Lifecon Deliverable D3.2*. 2003.

[21] Mark G. Stewart and David V. Rosowsky. "Time-dependent reliability of deteriorating reinforced concrete bridge decks". In: *Structural safety* 20.1 (1998), pp. 91–109. ISSN: 0167-4730.

[22] RK Dhir, MR Jones, and MJ McCarthy. "PFA concrete: chloride-induced reinforcement corrosion". In: *Magazine of Concrete Research* 46.169 (1994), pp. 269–277.

[23] Philip S. Marsh and Dan M. Frangopol. "Reinforced concrete bridge deck reliability model incorporating temporal and spatial variations of probabilistic corrosion rate sensor data". In: *Reliability Engineering & System Safety* 93.3 (2008), pp. 394–409. ISSN: 0951-8320.

[24] Féderation internationale du béton. *fib Model Code for Concrete Structures 2020 - Final draft*. 2023.

[25] Aurelio Muttoni and Miguel Fernández Ruiz. "Shear strength of members without transverse reinforcement as function of critical shear crack width". In: *ACI Structural Journal* 105.2 (2008), pp. 163–172.

[26] European Committee for Standardization. *FINAL DRAFT Eurocode 2: Design of concrete structures - Part 1-1: General rules - Rules for buildings, bridges and civil engineering structures*. 2021.

[27] Kim A. Vu and Mark G. Stewart. "Predicting the likelihood and extent of reinforced concrete corrosion-induced cracking". In: *Journal of structural engineering* 131.11 (2005), pp. 1681–1689.

[28] European Committee for Standardization. *Eurocode 2 - Design of concrete structures - Part 1-1 : General rules and rules for buildings*. 2004.

[29] European Committee for Standardization. *Eurocode 2 - Design of concrete structures - Part 1-1 : General rules - Rules for buildings, bridges and civil engineering structures*. 2022.

[30] Eline Vereecken. "Applied Bayesian pre-posterior and life-cycle cost analysis for determining and optimizing the value of structural health monitoring for concrete structures". eng. PhD thesis. Ghent University, 2022, pp. XXXII, 406. ISBN: 9789463555791.

[31] Féderation internationale du béton. *Model Code for Service Life Design*. 2006.

[32] Joint Committee on Structural Safety. *JCSS Probabilistic Model Code - Part 2 - Load Models*. 2001.

[33] J. Maljaars R. de Vries R.D.J.M. Steenbergen. "Annual reliability requirements for bridges and viaducts". In: *Heron Journal* 68.2 (2023), pp. 91–122.

Signature

TNO › Mobility & Built Environment › Delft › 22 January 2025

Ir. H.J.J. Weijs
Author

A. Höllbacher MBA
Project manager

Ir. M. van Roermund
Research manager

Appendix A

Implementation verification

The reliability assessment is determined through a Python script. The pseudo code for the assessment is shared in Chapter 3. In this annex, the same assessment is performed using an alternative method to calculate the probability of failure. The code is written in Python version 3.11.

The key difference between the pseudo code that is used to verify the calculation and the original script is that in this script in each time step every section is evaluated, whereas in the original script, for each section every year was evaluated.

The advantage of this script is that it is easier to understand, as it follows a chronological pattern. The advantage of the other script is that calculations are much quicker, because Python packages are used in a more efficient way.

A.1 Numerical Implementation

The sampling of the variables has not changed. That is why this pseudo code starts at the start of the calculation. The same holds for the calculation of the probability of failure.

```
results = empty list

FOR simulation in total number of simulations:

    SET t = 0
    SET t_final = 200

    WHILE t < t_final:
        FOR each section in beam:
            CALCULATE external effects:
                bending moment
                shear force

            CALCULATE capacity_function:
                bending moment
                shear force

            CALCULATE chloride concentration

            IF corrosion_concentration > critical_value:
                CALCULATE corrosion_degradation
                UPDATE capacity_functions:
                    bending moment
                    shear force

            CALCULATE limit_state_functions:
```

```
            bending moment
            shear

        IF any limit_state_function < 0:
            ADD failure_year, failure_location, failure_mode to results

            IF corrosion_concentration > critical value:
                ADD year_of_initiation to results
            ELSE:
                year_of_initiation = inf
                ADD year_of_initiation to results

            END

        ELSE:
            t = t+1

failure_year = inf
failure_location = None
failure_mode = None
year_of_initiation = inf

ADD failure_year, failure_location, failure_mode, \
    year_of_initiation to results
```

A.2 Results

Figure A.1 presents the comparison between the original implementation and the verification implementation. As can be depicted from this figure, the result yields the same conditional reliability for lower (<4) indices. Because two different approaches have resulted in the same outcome, the results are thereby verified.

Differences in the outcome, which are present for higher reliability indices, are the result of unconverged results. As explained in chapter 7, the calculation is not yet converged. The verification analysis is performed with fewer ($\approx$ 550k) simulations, which explains why the results diverge for an increasing reliability index. If more (e.g. 100M) simulations are performed, the outcome is expected to be identical.

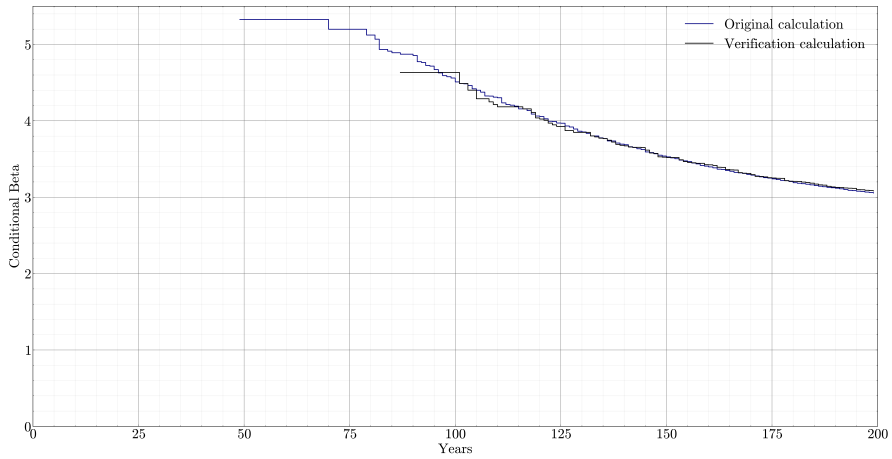

Figure A.1: Verification of the numerical implementation.

Mobility & Built Environment

Molengraaffsingel 8
2629 JD Delft
www.tno.nl

TNO innovation for life

TNO innovation for life

State of the art and literature review on chloride-induced corrosion

Reliability based life-time estimation of existing concrete structures in marine environments

TNO Intern ⟩ TNO 2025 R10108
14 January 2025

Mobility & Built Environment
www.tno.nl
+31 88 866 20 00

TNO 2025 R10108 – 14 January 2025

Reliability based life-time estimation of existing concrete structures in marine environments

State of the art and literature review on chloride-induced corrosion

Authors	Gina Torres-Alves Harrie Weijs Henco Burggraaf
Technical Review	Filipe Pereira Pedrosa
Vastgesteld d.d.	
Aantal pagina's	40 (excl. voor- en achterblad)

Summary

In the Netherlands, extensive water ways and hydraulic structures safeguard a significant portion of the country with regard to flood safety. These structures also enable water-based transport and the distribution of freshwater. Many of these structures were (partly) constructed out of reinforced concrete (RC), which is vulnerable to durability challenges, particularly in marine environments, due to the potential corrosion of embedded reinforcing steel. This corrosion can ultimately compromise the load-bearing capacity of the structures over time.

The main focus of this report is on the initiation phase of chloride-induced corrosion—the stage at which chlorides first penetrate the concrete and reach the steel reinforcement, starting the corrosion process. Nevertheless, a brief discussion also addresses the importance of the corrosion propagation phase in which the corrosion products expand, inducing stress and potential cracking in the concrete, which further affects structural performance. Details on how these two corrosion processes were implemented for modelling and the quantification methods of their respective parameters are presented in a separate report.

It is essential to understand chloride-induced corrosion and its effects on the long-term safety of these structures for estimation of their remaining life time. This report presents a literature review on the time-dependent reliability of non-cracked RC structures under chloride-induced corrosion. Accurate forecasting of the durability and longevity of hydraulic structures, contributes to enhancing flood safety, reducing costs, and supports efficient infrastructure planning. The insights obtained from this literature review have the potential to be of interest for broader environmental and economic perspectives.

Table of Contents

1 Introduction

1.1 The Dutch water engine

The Netherlands is renowned for their relationship with water, deeply influenced by its geographical positioning along the coastline and serving as the point where two significant European rivers, the Meuse and the Rhine, flow into the North sea. Water has been a key factor in the evolution of the country. Since from the 14th century, land reclamation from the sea and rivers began, while between the 16th and 18th centuries, maritime exploration expanded, leading to substantial wealth accumulation and advancements in scientific development. In the 17th century they experienced a Golden Age, where they were one of the most prosperous countries in Europe.

The relationship between the Netherlands and water was not without its drawbacks. The country is susceptible to both river and sea flooding. Multiple instances with over 10,000 casualties have been reported. One flood even resulted in over 100,000 lost lives. The most recent flood event happened in 1953. This flood, known as the 'Waternoodsramp' resulted in over 2500 casualties.

The Delta Works

The Delta works project emerged as a response to this flood, constituting a series of construction projects primarily situated in the southwestern part of the country aimed at protecting the land from flooding, particularly from the sea. These projects, developed in the latter half of the 20th century, included various structures such as dikes, dams, and storm surge barriers. The storm surge barriers, renowned globally, stand as unique structures capable of serving multiple purposes. Beyond their primary function of providing protection, these barriers can also regulate water levels and detain freshwater, among other functions.

1.2 Problem statement

Any structure should withstand the most severe conditions expected during its design operational lifespan with sufficient reliability. The replacement of hydraulic structures would incur costs amounting to billions of euros. Additionally, the initiation, design, and construction of new structures would demand a significant duration of time, not discounting the necessary demolition of the existing structures. Therefore, it could be advantageous to explore potential methods for evaluating the end-of-life phase of these structures. Such an assessment might prove beneficial in extending the technical lifespan of these structures.

Reliability analysis

There are multiple possible reasons why a structure might fail. These possible reasons are called failure modes and they define the specific ways in which the structure can cease to meet its intended purpose. Each failure mode consists of a chain of events and causes that can lead to failure of a structure. When performing the reliability analysis of a structure it is necessary to identify the potential failure modes to understand their associated risks.

In general, a reliability assessment starts by clearly defining the problem at hand. For this purpose, it is key to identify the structure, its components, and their respective failure modes.

The next step is to determine the loads and environmental conditions to which the structure is exposed, as well as the resistance of the materials and components. Subsequently, a criterion for failure is established that can be represented by ultimate and serviceability limit states. The uncertainties associated with the parameters relevant to the chosen failure mode need to be identified and quantified. Finally, a probabilistic assessment is performed to investigate the safety of the structure.

Systematically determining the failure probability

A popular methodology in risk and reliability analysis of structures is fault tree analysis (FTA). FTA is a graphical method that breaks down the main event, known as the top event (i.e., system failure or structural collapse), into multiple basic events in a tree-like structure. Each brand of the tree represents a potential event or combination of events that could lead to the undesired outcome. This methodology is useful to analyze the relationship between various events and their probabilities of occurrence. Therefore, if the probabilities of occurrence of the basic events and the relationship between all events are known, then the probability of the undesired main (top) event can be calculated. Currently, the assessment of system safety concerning storm surge barriers (and estimation of failure probabilities) relies on the utilization of fault trees. However, FTA is not suitable for dynamic systems or time-dependent processes such as degradation. This is because FTA assumes independence between basic events, limiting the analysis.

1.3 Need for time dependent reliability assessments

The role of time-dependent processes

To correctly estimate the lifetime of a structure or structural element, a time-dependent reliability assessment needs to be performed. Failure modes are often time-dependent and correlated to other events. Some mechanisms are more sensitive to time dependencies than others and this could influence their probability of occurrence. A mechanism with an initial low chance of occurrence, especially one that is highly time-dependent, has the potential to exceed the probability of another mechanism that starts with a higher probability of occurrence but is less time-dependent. A distinct advantage of this methodology over fault tree analysis lies in its ability to encompass time dependencies between the variables of interest. As a result, is possible to estimate the remaining lifespan of a structure.

An illustrative example

Figure 1 shows this importance through an illustrative example. In this figure, two failure mechanisms (A and B) of a structure were determined. For each mechanism, the structural reliability is calculated as a function of time. At time $t = 0$, failure mechanism A is the dominant failure mechanism, as it has the lowest reliability. However, after about 35 years, failure mechanism B becomes the governing failure mechanism. Generally, structures are designed for lifespans up to 100 years or more, depending on the structure. Different failure mechanisms show different sensitivities to time variations. Therefore, it is necessary to include time dependencies in reliability assessments.

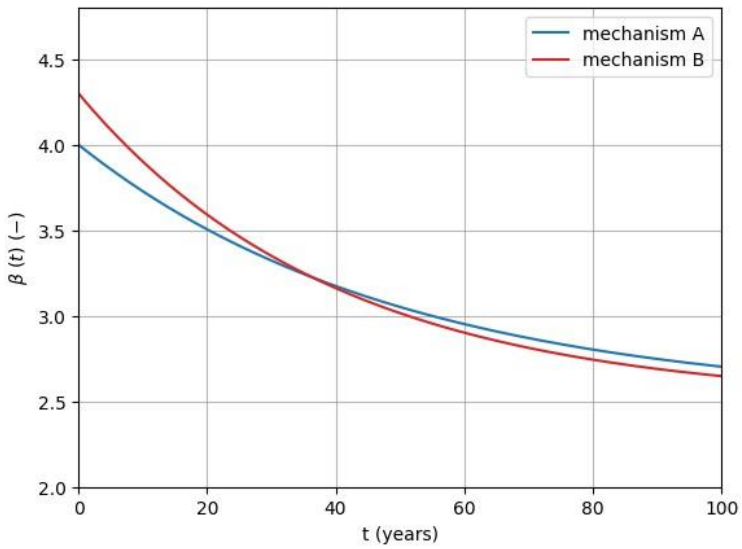

Figure 1 An illustrative example of the importance of including time dependencies in a reliability assessment.

1.4 Degradation of reinforced concrete structures in marine environments

Materials and components can show some form of deterioration over the years. This gradual deterioration or weakening over time can occur due to several factors such as environmental conditions, usage, and other external influences. This has an adverse impact on the reliability of structures. Incorporating degradation into the analysis can greatly enhance the reliability assessment of structures, providing a more accurate evaluation of their long-term performance and safety. This chapter discusses the steps for performing the probabilistic assessment of a structure. In one of these steps, degradation can be incorporated.

Storm surge barriers and other hydraulic structures located in coastal or marine environments can experience concrete degradation, more specifically, degradation due to chloride ingress. This saline environment leads to durability challenges, ultimately reducing the load bearing capacity of parts of the structure or even the entire structure, potentially leading to failure.

This report explores current models of chloride-induced corrosion through a literature review, with a particular focus on Dutch coastal environments. The main objective is to assess the reliability of structures located in these environments, taking into account the effects of time dependent deterioration. Instead of focusing in a particular structure, this report addresses chloride-ingress in general. It begins by defining the relevant limit states, followed by an introduction to various corrosion models and their connections with those limit states. The main variables within those models are quantified stochastically where possible (this is described in a separate report). The overall goal is to provide an overview of available model and variables relevant to time-dependent reliability assessments of structures in marine environments.

1.5 Structure of this report

In Chapter 2 the fundamental principles of time-dependent reliability are explained, focusing on time-dependent probability of failure and the calculation of the remaining service life. The concepts are the basis to understand how to model chloride-induced corrosion in concrete over time. Chapter 3 gives an overview of the state-of-the-art knowledge within TNO on service life prediction of concrete structures. Subsequently the model of reinforcement corrosion in non-cracked concrete due to chloride penetration is further investigated in Chapter 4, including chloride diffusion and the phases of chloride ingress. All models are based on Fick's 2nd law of diffusion. Chapter 5 presents the limit state functions and a literature-based review of parameters relevant to model corrosion. Finally Chapter 6 presents the conclusions and discussion of key findings.

2 Time dependent reliability

During its life a structure is subject to various environmental influences (e.g., moisture, temperature, chemical substances, biological processes, etc.) which, over time, may cause deterioration of the structure material(s). Deterioration usually influences both resistance and appearance of a structure, which means that safety and serviceability of the structure may be seriously compromised.

2.1 Time dependent probability of failure

In the case of deterioration the basic formula of the probability of failure within a certain period of time can be written as:

$$P_F = \int_{g[\mathbf{X}(t)]<0} f_{\mathbf{X}}(\mathbf{x})\, d\mathbf{x}$$

Eq. 1

X(t) is the vector of the basic random variables, in general time-dependent, which now includes in addition to mechanical load and resistance parameters also environmental parameters like chloride concentration, diffusion coefficients, degree of water saturation in concrete, etc. The limit state function g(.) includes the effects of deterioration on the resistance properties like strength and geometry. In many cases, P_F may be written as:

$$P_F = \mathrm{P}(g_1 < 0) + \mathrm{P}(g_2 < 0 \cap g_1 > 0) + \ldots$$

Eq. 2

$$g_k = R_k - S_k$$

Eq. 3

- R_k : Mechanical resistance at the end of the time period k, as a result of deterioration of the initial resistance;
- S_k: Maximum mechanical load within the time period k.

The limit states are SLS (serviceability) and ULS (collapse). However, for convenience, to deal with different aspects of deterioration, additional Condition Limit States like the initiation of corrosion or the propagation of corrosion are introduced (see ISO 2394 and ISO 13283). These condition limit states enable to refine/simplify the analysis of a deterioration process by considering various well-defined and controllable deterioration-related states, which are not associated with direct negative consequences. If done so, care should be taken to be on the conservative side, i.e., verify that the considered condition limit states do occur before the real limit states.

Modelling a deterioration process involves significant uncertainties associated with environmental conditions, material properties, limitations of predictive models, and inadequacy of material testing, detection, and inspection methods. In the next sections a state of the art is given on the probabilistic models needed for the reliability analysis of concrete structures subjected to chloride related degradation.

2.2 Reliability-based calculation of remaining service life time

The probabilistic assessment of the time-variant structural reliability allows evaluating the lifetime T* of the structure. It is the moment in time at which the actual reliability level of the structure will reach the target reliability level. This is illustrated in Figure 2.

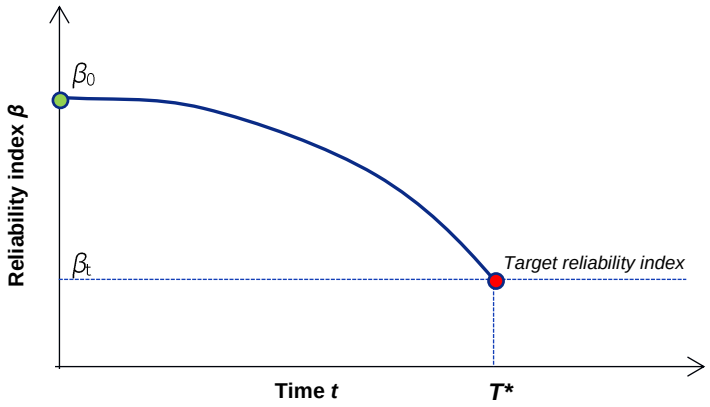

Figure 2 Definition of lifetime

Reaching the end of the remaining service life time does not necessarily mean that the structure requires strengthening, renovation or demolition. Instead, it may indicate that given the current state of information, it is not possible to accurately predict further into the future. Service life predictions improve when more detailed information is available (i.e new measurements), especially in degradation models. Large uncertainties in model coefficients can lead to a rapid decrease in reliability (Figure 2) resulting in a shorter service life. Reducing these uncertainties is beneficial, as shown in Chapter 5, where the differences between broadly applicable models with high uncertainty and more localized, structure specific models with reduced uncertainty are explored. Moreover, regular inspections can lead to an increased state of information and an update of the reliability (Figure 3). Although the calculations shown in Figure 3 are not part of this report, it is important to keep them in mind when setting up the probabilistic time dependent models.

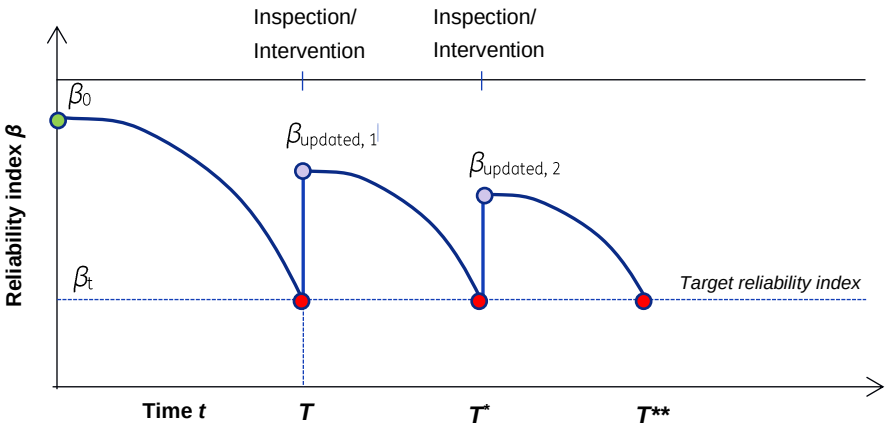

Figure 3 Updating reliability and life time extension through inspections. T*,T** correspond to the updated service life time.

3 State of the art service life prediction of concrete structures

This chapter gives an overview of the state-of-the-art knowledge within TNO on service life prediction of concrete structures regarding corrosion of reinforcement. Section 3.1 describes the relevant mechanisms that play a role. Section 3.2 presents the corresponding models for assessment.

3.1 Mechanisms

3.1.1 General

Steel exposed to the atmosphere (in the presence of oxygen and water) normally corrodes. However, in concrete steel is protected against corrosion. The corrosion protection of steel by concrete consists of both chemical and physical protection. The chemical protection is due to the high pH (alkalinity) in concrete, which causes so-called passivation of embedded steel. This yields a state without corrosion. Loss of passivation can develop due to carbonation of concrete around the steel and the presence of chloride ions at the steel surface. Depassivation gives a transition from the passive to the active state, in which corrosion and loss of metal can occur. These mechanisms will be discussed in further detail.

3.1.2 Carbonation

Carbonation is the reaction of carbon dioxide in the atmosphere with alkaline constituents in concrete. The pore solution in concrete mainly contains dissolved sodium and potassium hydroxides (NaOH, KOH), which gives a pH of 13 and higher. Carbonation turns these hydroxides into soluble sodium and potassium carbonates and solid calcium carbonate. Due to this mechanism the pH of the pore solution of concrete decreases to around 9 to 10.
When the carbonation front reaches the reinforcement, depassivation occurs and reinforcement starts to corrode. This corrosion takes the form of a more or less uniform distributed corrosion. The rate of carbonation depends on the concrete composition and the environment. Carbonation is promoted more in concrete with a moderate water content than in wet or dry concrete.

3.1.3 Chloride penetration

If chloride ions reach the reinforcement, depassivation can occur if the chloride content is above a so-called critical content. The critical chloride content depends on various factors including temperature, oxygen content and concrete composition. According to the latest insights, the probability of corrosion increases from low to high for increasing chloride contents between 0.2% and 1% mass per mass of cement.

Chlorides can be present in fresh concrete constituents (mixed-in chloride) or can penetrate into the concrete from the environment (penetrated chloride).
Corrosion due to chloride penetration usually takes the form of localised or pitting corrosion. Relatively small areas with active corrosion act as (small) anodes while the remaining steel surface acts as (large) cathode. Therefore corrosion rates can be high and pitting corrosion can be considerably more perilous than uniform corrosion.

3.1.4 Interaction of carbonation and chloride penetration

If concrete already contains some chlorides, carbonation accelerates the transport of chlorides through concrete. However, this effect is generally not very important because the proces of carbonation is normally slow. Also the conditions in which carbonation is promoted (semi-dry concrete, sheltered exposure) are opposite to the conditions in which chloride penetration is promoted (wet, fully exposed concrete).

Recent work has shown that carbonation also has a negative effect on the resistance against chloride penetration after a significant carbonation depth has been reached. In particular this is the case for carbonated blast furnace slag cement. Further study on this aspect is recommended.

3.1.5 Active corrosion

Active corrosion is the proces wherein iron atoms are oxidized and turned into iron ions. Poorly soluble corrosion products are formed that are more voluminous than the parent steel. This will lead to an expansion around the reinforcing bars which causes cracking and/or spalling at some point in time. This can be used as a warning sign, however attention should be paid to the fact that this only holds well for carbonation induced corrosion, already at an advance stage. Corrosion products originating from chloride induced corrosion are less voluminous and can be mobile, which will lead to less cracking and sometimes red-brown rust staining on the concrete surface.

Many parameters in the process of active corrosion are poorly known. Eventually the reduction of the rebar diameter can be such that the structural capacity may be influenced. In addition, cracking and spalling may have a negative effect on the bond between rebar and concrete.
For corrosion of prestressing steel, generally accepted predictive models are lacking. A first approximation can be obtained by applying models for corrosion of reinforcing steel. In addition to “normal” corrosion also stress corrosion cracking and hydrogen embrittlement are degradation mechanisms that may effect prestressing steel.

3.2 Models and assessment

3.2.1 General

This section deals with models for the mechanisms as described in section 3.1. In addition models for the assessment of existing structures are presented.

3.2.2 Carbonation

Models for the prediction of carbonation are given in DuraCrete (2000) and *fib* (2006). The carbonation depth in DuraCrete (2000) is given by:

$x(c) = \sqrt{(2\ C_{s,ca} * t / R_{ca})}$

With:
$x(c)$ = carbonation depth (m)
$C_{s,ca}$ = surface concentration (kg/m^3)
R_{ca} = carbonation resistance (years)

The carbonation resistance can be determined in an accelerated carbonation test, from:

$R_{ca} = R_{0,ca} / K_{ca} * (t_0 \div t)^{nca}$

With:
$R_{0,ca}$ = resistance from the compliance test at t_0 (s)
t = time (s)
nca = age coefficient (-)
K_{ca} = coefficient for effects of curing and environment:

$K_{ca} = k_{e,ca} * k_{c,ca}$

With:
$k_{e,ca}$ = environmental coefficient (-)
$k_{c,ca}$ = curing coefficient (-).

Values for the parameters can be obtained from (DuraCrete 2000).

The *fib* model for service life design (fib 2006) is similar to (DuraCrete 2000), but contains explicit functions for the effect of wetness and relative humidity. It is unknown to what level these functions have been verified.

In Burggraaf (2022a, b and c) the concrete of three Dutch storm surge barriers was assessed by TNO. In this research the carbonation depth was determined with:

$d(t) = C * \sqrt{t}$

With:
$d(t)$ = mean carbonation depth at time t (mm)
C = constant
t = exposure time (years)

For the concerning parts the constant in the expression above was determined as:

$C = d(t_1) / \sqrt{(t_1 - t_0)}$

With:
$d(t_1)$ = mean carbonation depth at time of measurement (mm)
$t_1 - t_0$ = time difference between measurement and start of exposition (years)

3.2.3 Chloride penetration

The models for corrosion due to chloride penetration are focussed on the transport of chloride from the environment to the reinforcement. These models assume that chloride penetrates by diffusion due to a gradient in concentration. The chloride content at the depth of the reinforcement is compared to a critical chloride content that is assumed to initiate corrosion.

In Burggraaf (2022a, b and c) a critical chloride content of 0.5% mass per mass of cement was used by TNO, based on practical experience in the assessment of existing structures. This value is in line with the value for the critical chloride content as included in CUR Recommendation 121:2018.

Examples of models to predict the chloride penetration are:
- DuraCrete model;
- *Fib* model;
- DuMaCon model;
- CUR guideline 1 model.

All these models are based on Fick's second law of (non-steady state) diffusion, assuming that the concrete microstructure does not alter due to interaction with the environment.

The DuraCrete model
The DuraCrete model combines the error function solution of Fick's second law of diffusion with a time dependent diffusion coefficient. The DuraCrete model is described in more detail in Chapter 4.

The fib model
The fib model (fib 2006) is based in the DuraCrete model. A difference with the DuraCrete model is that capillary absorption is taken into account by providing the chloride surface content C_s at the depth of its maximum. Another difference is that the temperature influence is taken into account. On the other hand the influence of execution is omitted.

The DuMaCon model
The DuMaCon model is developed during research on six coastal or marine structures in The Netherlands (Polder & Rooij 2005). The model is based on both the DuraCrete and *fib* model. A time dependent diffusion coefficient is incorporated, together with an environment depending surface chloride content and a fixed temperature factor. Also in this model an execution factor is omitted. The model was also developed for the assessment of existing marine structures.

The CUR Guideline 1 model
The CUR Guideline 1 model (CUR 2009) is based on the DuraCrete model with some modified parameters:
- A safety margin is applied to the cover depth;
- The diffusion coefficient must be tested using NTBuild 492;
- The chloride surface content C_s is not calculated, but is based on field data;
- The diffusion coefficient is multiplied by a correction factor to obtain the diffusion coefficient in a real structure (depending on binder type, environment and duration of wet curing).

3.2.4 Assessment of existing structures

In this section two examples of models for the assessment of existing structures are given:
- DuMaCon redesign model;
- CUR model for remaining service life.

DuMaCon redesign model
The DuMaCon redesign model is based on research on existing coastal and marine structures in the Netherlands (Polder & Rooij 2005). In this research a design model for new structures was derived, made using blast furnace slag cement. The model for existing (redesign)

structures is similar to the DuraCrete model, with input obtained from fitting chloride profiles from cores taken from the structure. The calibrated model can be used for making future predictions. Probabilistic calculations can be made by using statistical input variables.

CUR model for remaining service life
The CUR model for remaining service life is published in CUR-Recommendation 121:2018 "Bepaling ondergrens verwachte restlevensduur van bestaande gewapende betonconstructies" (CUR 2018). This CUR-Recommendation contains a procedure and a model.
The procedure involves the following:

1) Motivation for assessment of remaining service life. This can be:
   - Visual damage;
   - Increased risk profile;
   - Major maintenance (is it worth the costs);
   - Contractual obligation;
   - Transfer of ownership or maintenance.
2) Identification of critical elements. For this a preliminary investigation (structural analysis) is performed, making use of:
   - Design drawings and calculations;
   - As built drawings;
   - Results of previously performed inspections and investigations;
   - Information about comparable objects.
3) Visual inspection to identify damaged areas. During the visual inspection attention should be paid to:
   - Cracking;
   - Rust bloom;
   - (Indications of) leakages;
   - Spalled concrete;
   - Reinforcement corrosion.
4) Identification of condition of critical elements. Based on the results of the visual inspection it is determined which elements, if they fail, will have an adverse effect on the load-bearing capacity of the structure.
   In case of visible damage it should be determined, based on expert judgement, if damage is governing for the load bearing capacity or not. If it is governing, then a structural assessment according to NEN 8700 should be performed.
   In case of no visible damage a choice can be made between (i) having inspections carried out at a normal interval or (ii) determining the remaining service life. For determining the remaining service life the following steps for measurements should be taken:
   - Defining of test areas (≥ 6);
   - Cover depth measurements (≥ 12 per test area);
   - Core drilling (≥ 6 per test area);
   - Carbonation depth measurements per core;
   - Chloride analysis per core.

   The measurements should be processed using:
   - CUR 172 and CUR90-3 for carbonation;
   - The DuMaCon model for chloride penetration;
     The predicted time to corrosion is obtained on basis of a critical chloride content of 0,5% mass per mass of cement and two cover depths:
     i. The mean cover depth to obtain 50% probability of failure results;
     ii. The mean cover depth minus 5 mm to obtain 30% probability of failure results.

4 Modelling of reinforcement corrosion in non-cracked concrete

In this chapter, an overview is given of the state of the art models for chloride induced corrosion of concrete structures. In chapter 5, we will describe the probabilistic models for the input parameters.

4.1 General

Under normal conditions concrete protects the embedded reinforcing steel against corrosion, this is attributed to a passive oxide film that forms on the surface of steel in a highly alkaline environment provided by the concrete pore solution. There are two main causes that can disrupt the protective properties of concrete, i)carbonation or ii)penetration of chlorides (Rodríguez, Andrade et al. 2002). This study concentrates on chloride-induced corrosion, excluding carbonation from its scope, since this is the most common degradation mechanism for reinforced concrete structures (Pacheco and Polder 2016) in the Netherlands.

Chloride ingress typically results from external sources, such as structures situated in maritime environments, the usage of deicing salts or due to chloride-contaminated soils (DuraCrete 1998). Current models to describe chloride-induced corrosion rely on simplifying assumptions and are empirical. Mainly two categories of models are defined: i) empirical models, based on Fick's second law of diffusion, and ii) quasi-scientific models that describe certain aspects of the chloride penetration process. The main differences between these two categories depend on the input data requirements and model validation.

The mechanism of corrosion can be described in two stages (Tuutti 1982), i) initiation period, and ii) propagation period. The initiation period is defined as the stage between the first exposure of the RC structure to the environmental actions and the beginning of corrosion. This corresponds to the depassivation of the reinforcement due to the accumulation of chloride ions at the reinforcing steel layer. The propagation period is when corrosion occurs. In this stage, the structure deteriorates mainly due to reduction of steel cross-sectional area. This stage lasts until an unacceptable degree of corrosion damage has occurred, impacting the loading bearing capacity of the structure and/or its serviceability.

Most mathematical models that simulate chloride-induced corrosion focus on the initiation phase. In these models, the beginning of reinforced steel depassivation marks the end of the service life (Browne 1982, Funahashi 1990, Maage, Helland et al. 1995, Tang and Nilsson 2018). However, according to Rasheeduzzafar, Al-Saadoun et al. (1992), the safety of the structure is only diminished or impacted when there has been a large loss of the reinforced steel cross-sectional area or loss of bond at the steel-concrete interface. Design strategy for service life modeling related to corrosion of reinforcement typically uses initiation phase

models for the design of new structures and propagation stage models for the evaluation of structures already in service with corroding reinforcement (Martın-Pérez 1999). In this report, the main focus is on the initiation phase.

The assessment of reinforced concrete structures under chloride-induced corrosion highlights the significance of time dependent reliability. Chloride ions in non-cracked concrete gradually infiltrates the structure leading to corrosion and a progressive deterioration in structural integrity. For this reason, it is essential to recognize the time-dependent nature of corrosion. Taking into account factors such as the rate of chloride ingress, the evolving nature of corrosion products and its implications for structural safety, engineers can make informed decisions regarding maintenance, repair and rehabilitation practices. However, predicting the impacts of these factors deterministically can be challenging. Therefore, a probability-based methodology that accounts for uncertainties related to structural performance and loadings becomes crucial in ensuring structural safety and reliability. A time-dependent reliability approach may ensure the robustness of the structure leading to extending their service life and enhancing overall public safety. The following sections present a review of the general mathematical models and assumptions.

4.2 Chloride diffusion

Chloride ions from external sources can penetrate concrete via a combination of different transport mechanisms such as ionic diffusion, absorption of water containing chlorides, permeation, dispersion of diffusing chloride ions or by the movement of water through concrete exposed to water in one surface and dry on the other side (Martın-Pérez 1999). A great part of service life models regarding chloride-induced corrosion assume diffusion as the main transport mechanism (Martın-Pérez 1999). Thus, this report is focused on diffusion as the main transport mechanism for chlorides.

Ionic diffusion occurs because of a concentration gradient between the exposed surface and the pore solution of the cement matrix, under the assumption that the concrete is in a saturated state. This phenomenon can be described using Fick's 1st law of diffusion, which for a one-dimensional flow is:

$$J_c = -\ \bar{D}_c \frac{\partial C_{fc}}{\partial x}$$

Eq. 4

where:

J_c is the flux of chlorides due to diffusion in the x-direction (kg/m^{2}s^1):
$\bar{D}_c$ is the effective chloride diffusion coefficient (m^2/s):
C_{fc} is the concentration of chlorides dissolved in the pore solution (kg/m^3 of pore solution).

The negative sign in Eq.4 **Error! Reference source not found.** means that diffusion happens i n the opposite direction to that of increasing concentration. Note that the value of the diffusion coefficient $\bar{D}_c$ is different if C_{fc} is expressed in different units (Luping and Nilsson 1993, Jensen, Hansen et al. 1999). The dissolved chloride ions can also be given in terms of kg/m^3 concrete, resulting in a different effective chloride diffusion coefficient D_c:

$$\bar{D}_c = D_c \omega_e$$

Eq. 5

where:

ω_e is the evaporable water content expressed per unit volume of concrete, given the assumption that this is the water in which diffusion occurs.

Chloride ions can be present in three different forms (Neville 1995): (1) chemically bound to the hydration products of the cement; (2) physically sorbed on the surfaces of the gel pores; and (3) dissolved in the pore solution. The total chloride content is the sum of the bound (1, 2) and free (3) chlorides:

$$C_{tc} = C_{bc} + \omega_e C_{fc}$$

Eq. 6

where:

C_{tc} is the total chloride concentration (kg/m^3):

C_{bc} is the concentration of bound chlorides (kg/m^3).

The law of conservation of mass states that for any closed system the system's mass cannot change, i.e., it is conserved over time. This means that a change in diffusive flux needs to be balanced by a change in the amount of total chlorides in the system:

$$\frac{\partial C_{tc}}{\partial t} = \frac{\partial C_{bc}}{\partial t} + \omega_e \frac{\partial C_{fc}}{\partial t} = -\frac{\partial J_c}{\partial x}$$

Eq. 7

Fick's 2nd law of diffusion is found when chloride binding is neglected ($C_{bc} = 0$). This can only be neglected when diffusion in a solution is considered, instead of in a concrete (Nilsson 1996).

$$\frac{\partial C_{fc}}{\partial t} = \frac{\partial}{\partial x}\left(D_c \frac{\partial C_{fc}}{\partial x}\right)$$

Eq. 8

If the initial- and boundary condition are $C_{fc}(x > 0, t = 0) = 0$, and $C_{fc}(x = 0, t > 0) = C_s$ respectively, with C_s being the chloride concentration at the surface $x = 0$, the following closed-form solution is obtained:

$$C_{fc}(x,t) = C_s\left[1 - \mathrm{erf}\left(\frac{x}{2\sqrt{D_c t}}\right)\right]$$

Eq. 9

where:

$C_{fc}(x,t)$ is the concentration of free chlorides at depth x after time t (kg/m^3 of pore solution);

C_s is the chloride concentration at the surface $x = 0$ (kg/m^3 of solution);

erf is the error function.

t time of exposure (s)

Note that Eq. 9 only holds when both the surface chloride concentration C_s and the diffusion coefficient D_c are constant in space and time. However, D_c is a function of, among others, chloride-concentration, temperature, age of the concrete, binder content, micro crack density (proportion of micro-crack volume per unit volume of concrete), moisture content. C_s is a function of the concrete quality and the exposure conditions.

However, when the chloride coefficient is assumed as time-independent, the model results in unrealistic estimations of service life. Therefore, the constant coefficient of diffusion is replaced by a time-dependent material characteristic (Gehlen, Greve-Dierfeld et al. 2015):

$$D_{app}(t) = D_{app}(t_0) \cdot \left(\frac{t_0}{t}\right)^{\alpha}$$

Eq. 10

Where:

- $D_{app}(t_0)$: Apparent chloride diffusion coefficient determined at a reference time t_0 [m2/s]
- α : Aging exponent that indicates the decrease of the apparent chloride diffusion coefficient over time.
- $D_{app}(t)$: Always represent the diffusion coefficient of the concrete over the entire time period t as an averaged constant.

4.3 Modelling chloride ingress

According to DuraCrete (1998), models that aim at predicting the performance of reinforced concrete structures at the different stages of corrosion should have the following components:

- Prediction of the time-dependent ingress of aggressive agents.
- Prediction of the threshold that beyond it the aggressive agents cause loss of passivity.
- Define the initial depth of the cover to the embedded reinforcement and any reduction of the effective cover due to physical and chemical deterioration process.
- Prediction of the rate of corrosion of the reinforcement
- Prediction of the structural consequences of corrosion.

Most differences between models that characterize the initiation phase of chloride ingress relate to the chloride threshold. Factors that can influence this threshold are (DuraCrete 1998):

- Concrete mix properties
- Degree of compaction
- Cover depth
- Concrete/steel interfacial zone
- Nature and extent of cracking
- Source of chloride contamination
- Exposure environment

It is not always certain which of these factors is the dominant one. Current models can be classified into two categories: empirical models, and quasi-scientific models. The main difference between these categories lie in their input data, data requirements and validation methods. Empirical models are based on modified versions of Fick's 2nd law of diffusion (Section 4.2) and the quasi-scientific models rely on a scientific approach in modelling specific aspects of the chloride penetration process (DuraCrete 1998). This report focus on the empirical models.

Empirical models are based on the assumption that the phenomena that describes chloride ingress manifest in a chloride penetration coefficient (D_a). This coefficient varies with the duration of the exposure and the depth of penetration (DuraCrete 1998). Moreover, empirical models are derived from data of inspected structures. Thus, it is important to consider that these models might not be flexible enough to include conditions outside of the scope of the available data used in their development.

To generate models that are able to predict the onset of corrosion in concrete, is necessary to (DuraCrete 1998):

- Derive formulas that represent the nature of the process (previous section)
- Perform sensitivity analyses to determine the critical parameters in the model
- Generate input data (laboratory or field observations)
- Evaluate the accuracy of the models by comparing predicted behavior with field/lab performance.

In the following section, a summary of models for chloride ingress is presented.

4.3.1 Initiation phase

In this section, a summary of models that consider the prediction time on the onset of chloride-induced corrosion is presented. As mentioned in previous sections, chloride ingress in concrete is the result of the complex interaction of different processes that after a certain time of exposure result in chloride concentration profile (DuraCrete 1998). This profile shows the distribution of chloride content with respect to the depth from the concrete surface. Related empirical models are briefly described next.

4.3.1.1 Modelling with age-dependent diffusion coefficient

This model is proposed by Poulsen (1993) that combined the differential equation of uniaxial diffusion into an isotropic medium presented by Crank (1979) with suitable boundary conditions. The model considers the age dependency of the chloride diffusion coefficient, assuming a surface chloride level, as follows:

$$C(x,t) = C_i + (C_{sa} - C_i)\,\mathrm{erfc}\left(\frac{x}{\sqrt{4(t-t_{ex})D_a(t)}}\right)$$

Eq. 11

Where:

- $D_a(t)$: Function describing the age-dependency of the achieved chloride diffusion coefficient.

D_a with respect to initiation at a specific time t_0 is computed as:

$$D_a(t_o) = \frac{c_d^2}{t_0 \xi_{cr}^2}$$

Eq. 12

ξ_{cr} is defined as:

$$\xi_{cr}^2 = 2\ \mathrm{erf}\left(\frac{C_{cr} - C_i}{C_{sa} - C_i}\right)^{-1}$$

Eq. 13

If $D_a(t)$ is known, the value corresponding to the design stage $D_a(t_{ex})$, can be obtained.

(Bamforth 1994, Mangat and Molloy 1994, Bamforth 1995, Maage, Helland et al. 1995, Poulsen 1995, Bamforth 1999) use the following expression for $D_a(t_{ex})$:

$$D_a(t_{ex}) = D_a(t_0)\left(\frac{t_{ex}}{t_0}\right)^{-n}$$

Eq. 14

Where:

- n governs the age-dependency. It depends on the type of concrete and exposure conditions. The chosen value of N should be done with caution.

4.3.1.2 Modelling with age dependent surface chloride level

These type of models describe the chloride accumulation as being proportional to the square root of time, as follows:

$$C(x,t) = C_i + S_1\sqrt{t - t_{ex}}\left[exp(-z^2) - z\sqrt{\pi} \cdot \mathrm{erfc}(z)\right]$$

Eq. 15

Where:

$$z = \frac{x}{\sqrt{4(t - t_{ex})D_a}}$$

Eq. 16

The equation can also be written as:

$$C(x,t) = C_i + S_1\sqrt{t - t_{ex}}\,\Psi_{0.5}(z)$$

Eq. 17

Where:

- $\Psi_{0.5}(z)$ is a mathematical function whose values are given in standard tables (Mejlbro 1996).

- S_1 is the concrete's surface chloride concentration after 1 year of exposure. Calculated as follows:

$$S_1 = \frac{C_{sa}(t_{in}) - C_i}{\sqrt{(t_{in} - t_{ex})}}$$

Eq. 18

- $C_{sa}(t_{in})$ and D_a are obtained by applying the best fit curve to the achieved chloride profile at time of inspection, using 17.
- D_a is calculated as follows:

$$D = \frac{c_d^2}{t_0 \chi_{cr}^2}$$

Eq. 19

Where:

$$\chi_{cr} = 2\Psi_{0.5}^{-1}\left(\frac{C_{cr} - C_i}{S_1\sqrt{t_0}}\right)$$

Eq. 20

$\Psi_{0.5}^{-1}$ is the inverse of the $\Psi_{0.5}(z)$ function.

S_1 may be estimated from chloride profiles achieved after 1 year of exposure or from experience. The build-up of surface chloride levels can be modelled as:

$$C_{sa}(t) = S_1 t^p$$

Eq. 21

By choosing a suitable value for "p" within the range of 0 to 1, it is possible to achieve a closer alignment with the trends observed in reality.

A solution is provided by (Mejlbro 1996):

$$C(x,t) = C_i + S_1 t^p \, \Psi_p(z)$$

Eq. 22

Where:

$$z = \frac{x}{\sqrt{4tD_a}}$$

Eq. 23

This is valid only for $t_{ex} = 0$, $C_i = 0$ and for a time dependent D_a.

There are tables where the values of the $\Psi_p(z)$ function can be found (Mejlbro 1996).

4.3.1.3 Modelling with age-dependent diffusion coefficients and surface chloride contents

Mejlbro (1996) solved the differential equation of uniaxial diffusion into an isotropic medium. This was accomplished with an age-dependent penetration coefficient, alongside the representation of the time-dependent increase in surface chloride levels using a set of functions formulated as follows:

$$C_{sa} = C_i + S_1 \cdot \{(t - t_{ex}) \cdot D_a(t)\}^p$$

Eq. 24

Where p>0. The solution is given by:

$$C(x,t) = C_i + S \cdot \{(t - t_{ex}) \cdot D_a(t)\}^p \cdot \Psi_p\left(\frac{x}{\sqrt{4(t - t_{ex})D_a}(t)}\right)$$

Eq. 25

That is also written as follows:

$$C(x,t) = C_i + S \cdot \left(\frac{x}{2}\right)^{2p} \cdot \Lambda_p\left(\frac{x}{\sqrt{4(t - t_{ex})D_a}(t)}\right)$$

Eq. 26

Mejlbro (1996) provides tables for which the values of the $\Psi_p(z)$ and $\Lambda_p(z)$ functions can be obtained.

4.3.1.4 Modelling with variable diffusion coefficient depending on depth, time and chloride concentration

Based on the application of the Boltzmann-Matano method, Tumidajski, Chan et al. (1995) developed an approach to calculate the transient diffusion coefficients, in other words, the diffusion coefficients are calculated as a function of time of exposure, penetration and chloride concentration. This reflects the dynamic nature of the diffusion process rather than assuming a fixed rate.

With the Boltzmann variable $u = x/\sqrt{t}$, the differential equation of uniaxial diffusion into an isotropic medium is transformed to a homogeneous differential equation. This is an equation that no longer depends on the spatial coordinate x or the time variable t separately, instead depends on a single combined variable u. An expression for the concentration dependent diffusion is derived:

$$D(C^*) = \frac{-1}{2T} \cdot \left(\frac{dx}{dC}\right)_{C^*} \cdot \int_0^{C^*} x\, dC$$

Eq. 27

The chloride profiles are fitted to the following equation:

$$C = A \cdot e^{-Bx}$$

Eq. 28

Where:

- A,B are constants. Their values are determined (for each profile) by minimizing the chi-squared values using the Levenberg-Marquardt algorithm.
- C is the concentration of chloride.

The chloride diffusion coefficients can be calculated with Eq. 27.

Tumidajski, Chan et al. (1995) also developed a method for forecasting the diffusion coefficient at any given penetration depth and exposure duration, for different concrete types and environmental conditions. This method involves plotting the calculated diffusion coefficients (logarithmically) against the Boltzmann variable, followed by regression analysis to derive the constants A and B in Eq. 29:

$$\log D = A + B \cdot \left(\frac{x}{\sqrt{t}}\right)$$

Eq. 29

x is in cm and t in months.

4.3.1.5 Modelling skin effects

Chloride profiles in field structures frequently exhibit deviations from the ideal profile shape, primarily within the near-surface concrete layer. Andrade, Díez et al. (1997) proposed that this phenomenon, often called the "concrete skin effect," can be conceptualized by treating the concrete as consisting of two distinct layers: a surface concrete skin with a diffusion coefficient D_1 and a subsurface layer with a different diffusion coefficient D_2. This model can be mathematically expressed using Eq. 30 and Eq. 31, as originally presented by Crank (1979).

$$C_1(x,t) = C_s \sum_{n=0}^{n=\infty} \alpha^n \left(\operatorname{erfc}\left[\frac{(2n+1)lx}{2\sqrt{D_1 t}}\right] - \alpha \operatorname{erfc}\left[\frac{(2n+1)l - x}{2\sqrt{D_1 t}}\right]\right)$$

Eq. 30

$$C_2(x,t) = \frac{2kC_s}{k+1} \cdot \sum_{n=0}^{\infty} \alpha^n \operatorname{erfc}\left[\frac{(2n+1)l + kx}{2\sqrt{D_1 t}}\right]$$

Eq. 31

Where:

- $C_1(x,t)$: chloride concentration at time t in the concrete skin (-1<x<0)
- $C_2(x,t)$: chloride concentration at time t in the subsurface layer (x>0)
- D_1: Diffusion coefficient at the surface of the concrete skin
- 1 : thickness of the skin
- k and α are given by:

$$k = \sqrt{D_1 / D_2}$$

Eq. 32

$$\alpha = \frac{1-k}{1+k}$$

Eq. 33

The model is valid provided that D_1, D_2, C_s and the thickness of the concrete skin (l) are independent of time and that no chlorides are initially present in either layer.

4.3.1.6 Modelling edge effects

There are relatively few models that consider the two-dimensional aspects of diffusion, particularly in corner regions. Additionally, no effort has been dedicated to verifying these models against observed phenomena. In cases where the diffusion coefficient remains constant over time, and the concrete is presumed to be isotropic (a property of concrete where its physical properties are uniform in all directions). Thus, this results in chloride ions diffusing at the same rate in any direction. The following two-dimensional partial differential equation is applicable:

$$\frac{\partial C}{\partial t} = D\left[\frac{\partial^2 C}{\partial x^2} + \frac{\partial^2 C}{\partial y^2}\right]$$

Eq. 34

An analytical solution for this equation is available under the assumptions of quasi-homogeneous concrete (when concrete is assumed to have a nearly uniform properties throughout, but there might be small variations that are not significant enough to affect the overall diffusion process), a time-independent surface chloride level, and the absence of initial chloride content, as outlined by Crank (1979):

$$C(x,y,t) = C_{sa} \cdot \left[1 - \operatorname{erfc}\left(\frac{x}{2\sqrt{D_a t}}\right) \cdot \operatorname{erfc}\left(\frac{y}{2\sqrt{D_a t}}\right)\right]$$

Eq. 35

More general cases can only be treated numerically, for example using finite element methods to estimate the effect of structural shape and chloride binding on the initiation process.

4.3.2 Propagation phase

The service life of reinforced concrete (RC) structures concerning reinforcement corrosion is modeled in distinct phases, following predefined limit states related to corrosion-induced damage. Initially conceptualized by Tuutti (1982), the service life consists of a corrosion initiation phase (t_i) and a corrosion propagation phase (t_p), with the total service life expressed as $t_{service} = t_i + t_p$. However, Tuutti's model does not adequately represent the various sub-phases within the propagation phase (Li 2004).

The duration of the propagation phase depends primarily on the corrosion rate, which is influenced by multiple factors such as w/c ratio, temperature, chloride io concentration, moisture content in concrete, concrete permeability, among others (Živica 2003, Scott and Alexander 2007, Otieno, Alexander et al. 2010). The quantification of the corrosion rate on

reinforcement steel bars can help the prediction of the residual life time (Nieves-Mendoza, Gaona-Tiburcio et al. 2012).

The deterioration caused by corrosion has a negative effect on the structural and durability performance of RC structures. Predicting corrosion propagation is a complex task due to the challenge of incorporating all relevant factors into a prediction model. Typically, one type of corrosion-induced damage is adopted as a limit state in these models, signaling the end of the corrosion propagation period. Potential damages range from loss of steel cross-section (Stansbury and Buchanan 2000), loss of stiffness (Xia and Brownjohn 2003), loss of steel–concrete interface bond [17], and cracking of the concrete cover to global structural failure. However, is important to consider safety concerns if global failure is used as limit state.

A corrosion propagation prediction model can be developed based on various corrosion damage indicators, but current models typically focus on a single damage indicator. Prediction models can be classified into three main categories: empirical, numerical, and analytical models.

- **Empirical Models:** These models are based on direct relationships between corrosion rates and basic concrete parameters, for example, water-to-binder ratio, binder type (Bjegović, Krstić et al. 2006). They are usually derived from controlled laboratory experiments that isolate influencing parameters. Three sub-types exist:
    - Expert Delphic Oracle Models: Rely on past experiences to estimate corrosion rates but have not been widely used for chloride-induced corrosion due to their complexity.
    - Fuzzy Logic Models: Use fuzzy set theory[1] to define relationships between parameters and estimate corrosion rates (Sobhani and Ramezaninpour 2009). They have been applied to assess corrosion-induced deterioration and estimate reductions in steel cross-sectional area (Bjegović, Krstić et al. 2006).
    - Electrical Resistivity Models: Assume that concrete's electrical and oxygen diffusion resistance are key factors influencing corrosion (Scott and Alexander 2007).

A limitation of empirical models is their isolation of variables, which may not accurately represent real-world interactions, potentially leading to inaccurate service life estimations.

- **Numerical Models:** These models use mathematical equations to approximate the behavior of RC structures over time (Warkus, Brem et al. 2006, Scott and Alexander 2007). They can estimate corrosion rates and structural responses to damage and include:
    - Finite Element Method (FEM): Allows to model the entire structure, accounting for interfacial properties and changes in material properties over time (Zhu 2013). However, these models can become computationally expensive and time-consuming.
    - Boundary Element Method (BEM): Focuses on the concrete-steel interfaces and requires fewer elements than FEM, but assumes constant electrolyte

[1] Mathematical framework that treats uncertainty, it allows the variables to belong to sets with various degrees of membership, rather than being strictly classified as in or out.

conductivity and can only compute results at discrete points (Warkus, Brem et al. 2006).
    - Resistor Networks and Transmission Line Models: Represent corrosion processes using electrical circuit analogies, focusing on voltage, resistance, and current relationships (Raupach 1996).

- **Analytical Models:** These models provide solutions to mathematical equations that describe the corrosion process. They often use a thick-walled cylinder approach to model cracking and bond degradation (Chun-Qing, Melchers et al. 2006). However, these models can be faced with non-linear behavior and require calibration using experimental data.

This section provides a general overview of the propagation phase of corrosion and the main categories of models used for this purpose. A more detailed examination of the specific models chosen in our implementation to simulate corrosion propagation in non-cracked reinforced concrete structures will be presented in the follow-up report. This subsequent report will introduce each selected model, outlining the variables considered and detailing the assumptions made to quantify the necessary parameters.

5 Limit State Functions and Literature-Based Parameter Review for Corrosion in Reinforced Concrete Structures

In this chapter focus is on defining limit state functions and detailing statistical parameters for corrosion models.

The literature review includes various sources, with special attention on the DuMaCon study by Polder and de Rooij (2004), where a series of investigations was carried out on six concrete structures along the North Sea coast in The Netherlands and proposed a probabilistic model for prediction of corrosion initiation in Blast Furnace Slag Cement concrete in marine environments.

5.1 Limit state functions

In cases that involve chloride-induced corrosion, it is assumed that the depassivation of the reinforcement takes place once a critical chloride content (action) capable of inducing corrosion has penetrated to the depth of the reinforcement. Consequently, the condition limit state equation is as follows (Gehlen, Greve-Dierfeld et al. 2015) :

$$g(X,t) = C_{crit} - C(c,t)$$

Eq. 36

Alternatively:

$$g(X,t) = c - x_{crit}(c,t)$$

Eq. 37

Where:

- X: Vector with random variables.
- $x_{crit}(t)$: depth at which a critical, corrosion-inducing chloride content is reached at time t [mm]
- c: concrete cover [mm]
- C_{crit}: Critical corrosion-inducing chloride content. It is an assumed threshold that depends on the thickness and quality of the concrete cover (resistance), and the

chloride content at the level of the layer of the embedded reinforcement at time t $C(x = c, t)$ as the action.

If is Eq. 36 expanded to model with age-dependent diffusion coefficient with Eq. 11, Eq. 12, and Eq. 13, then:

$$g(X,t) = C_{crit} - \left[C_i + (C_{sa} - C_i)\,\mathrm{erfc}\left(\frac{x}{\sqrt{4(t - t_{ex})\dfrac{c_d^2}{t_0\left(2\ \mathrm{erf}\left(\frac{C_{crit} - C_i}{C_{sa} - C_i}\right)^{-1}\right)}}} \right) \right]$$

Eq. 38

Where:

- C_{sa} achieved surface chloride content (this is a best fit, and not, a true value)
- erf is the error function
- C_i is the background chloride concentration
- t_{ex} is the time of first exposure
- t exposure period
- c_d cover depth

Given that corrosion is a progressive phenomenon that unfolds over time, it is crucial to acknowledge its time-dependent characteristics. Considering factors mentioned in the preceding chapter, such as chloride content, concrete cover, etc. underscores the importance of incorporating time-dependent reliability into the evaluation of the remaining service life of reinforced concrete structures. In the following sections, a comprehensive exploration of the stochastic variables associated with modelling of chloride-ingress are discussed, given the limit state function presented in Eq. 36. Quantification of these variables is crucial for accurately assessing the overall reliability of reinforced concrete structures.

5.2 Critical chloride content C_{crit}

The critical chloride content C_{crit} (percentage mass over cement weight, or wt.-%/b) is a threshold value, beyond which reinforcement steel depassivation starts. As discussed in chapter 4, this does not immediately lead to a loss of load bearing capacity. The onset of steel depassivation therefore represents a limit state with respect to maintainability.

Breit (2001) investigated the critical chloride content and found a lower bound of 0.2 wt.-%/b. This threshold consistent across various test methods, conditions, and chemical method used to determine it.

When determining the distribution of C_{crit}, it is usually assumed that the left tail of the distribution is bounded. However, in DuraCrete, Brite et al. (2000) suggest a normally distributed C_{crit} value of 0.48±0.15 wt.-%/b, implying about a 3% chance of finding values lower than 0.20. The chances of finding a value lower than 0 are almost negligible (about 0.01%). The studies in DuraCrete (1998) mainly focus on Portland cement (PC) types.

Edvardsen and Mohr (1999) propose a value of 0.9±0.15 wt.-%/b (normal distributed), without detailing the basis for this parameter. It appears they may have chosen it arbitrarily, as it is only presented within a numerical example.

Izquierdo, Alonso et al. (2004) performed chloride penetration tests by applying a voltage difference under submerged conditions with different water/cement ratios (0.5, 0.4 and 0.3). They found that a lognormal distribution best describes C_{rit}, with mean values of 1.5, 2.0 and 2.2 wt.-%/b, respectively, and a coefficient of variation of 0.36, independent of the water/cement ratio. Higher water/cement ratios relate to lower mean values. PC was used in this study.

Most studies on the critical chloride content are related to PC. This is acknowledged in Polder and de Rooij (2004), where a need for research of blast furnace slag (BFS) cement types is recommended, since this is commonly used in marine environments along the Dutch coast. In this study, they assumed a deterministic value of $C_{rit} = 0.50$ wt.-%/b which was identical to the critical chloride content for a PC-structure with a w/c of 0.45.

Pacheco and Polder (2016) made an attempt to determine the critical chloride content of BFS-based concrete. They performed a chloride penetration test on reinforced PC and BFS cement specimen for 6 months, continually monitoring the chloride content. At the end of the exposure period, all PC samples were corroded, while none of the BFS specimen did, despite that PC specimen (15 mm) were given a larger cover than BFS specimen (10 mm). For PC they found an average wt.-%/b value of 0.56, which is in line with other literature. BFS specimen yielded chloride concentrations lower than 0.1 wt.-%/b. They concluded that BFS specimen outperform PC cement types with regard to the critical chloride content.

Gehlen, Greve-Dierfeld et al. (2015) present a value of 0.60±0.15 wt.-%/b (beta distributed, with $a = 0.2,\ b = 2.0$). This value is adopted in *fib* Bulletin 34 (fib 2006), where it is recommended for ordinary mild steel. Other steel qualities show different values for the parameters related to the beta distribution. Table 5.1 presents an overview of the above mentioned.

Table 5.1: Distribution types and parameters for C_{crit}.

Source	Distribution type	Cement type	w/c ratio (-)	Mean (wt.-%/b)	Coefficient of variation (-)
DuraCrete	N	PC	0.20 – 0.80	0.48	0.31
Edvardsen and Mohr	N	-	-	0.9	0.17
Izquierdo et al.	LN	PC	0.3; 0.4; 0.5	1.5; 2.0; 2.2	0.36
DuMaCon	D	BFS	0.45[1]	0.5[1]	-
Gehlen	Beta a=0.2, b=2.0	-	-	0.6	0.25

[1] Since data about C_{crit} is lacking for BFS, they used the value that they found for PC. This structure had a w/c ratio of 0.45. N=Normal (Gaussian distribution). LN=LogNormal distribution. D=Deterministic.

5.3 Chloride diffusion coefficient D_c

At the concrete-water interface, the chloride content is higher than at the concrete-reinforcement interface. This gradient results in a flux of chloride-ions in the opposite direction. The rate at which this happens is described by the chloride diffusion coefficient D_c. This parameter is time dependent, i.e., $D_c = D_c(t)$.

DuraCrete, Brite et al. (2000) concluded that, based on 8 Dutch measurements of CEM III/B samples, a value of 2.0±0.15 (10^{-12} normal distributed) best describes D_c. The measurements contain a cement content of 300 kg/m^3 and a w/c ratio of 0.45.

Polder and de Rooij (2004) and JCSS Probabilistic Model Code (2020), both propose a RCM-test to determine the diffusion coefficient. This results in a diffusion coefficient $D_{RCM,0}$ at a reference time t_0 and can be transformed to the apparent diffusion coefficient $D_a(t)$ through Eq. 39.

$$D_a(t) = D_{RCM,0}\left(\frac{t_{ref}}{t}\right)^{\alpha}$$

Eq. 39

Where α is the age exponent (see section 5.6). D_a does not represent a physical property of concrete at a particular time, but rather an average diffusivity over a time period t. When the time period changes, D_a also changes. If no data is present, Table 5.2 can be used to quantify $D_{RCM,0}$.

Table 5.2: Quantification of $D_{RCM,0}$ for different concrete mixtures (extracted from *fib* Bulletin 34 (fib 2006).

	$D_{RCM,0}$ (10^{-12} m^2/s)					
Cement type	w/c$_{eqv}$[1]					
	0.35	0.40	0.45	0.50	0.55	0.60
CEM I 42.5 R	n.d.[2]	8.9	10.0	15.8	19.7	25.0
CEM I 42.5 R + FA (k=0.5)	n.d.[2]	5.6	6.9	9.0	10.9	14.9
CEM I 42.5 R + SF (k=2.0)	4.4	4.8	n.d.[2]	n.d.[2]	5.3	n.d.[2]
CEM III/B 42.5	n.d.[2]	1.4	1.9	2.8	3.0	3.4

[1] equivalent water-cement ratio, hereby considering FA (fly ash) or SF (silica fume) with the respective k-value (efficiency factor). The considered contents were: 22 wt.-%/cement; SF: 5 wt.-%/cement.

[2] n.d. – chloride migration coefficient $D_{RCM,0}$ has not been determined for these concrete mixes

5.4 Chloride surface content C_s

The chloride surface content is the average concentration of chloride-ions at the surface interface between the concrete and the sea water. For structures in submerged zones, C_s can assumed to be constant.

According to Joint Committee on Structural Safety (2020), the value of the surface content can be taken as 2.5±0.38 wt.-%/b (normal distributed) when the surface is submerged. They base this on various sources, most of which are based on PC with a w/c ratio of around 0.40.

Polder and de Rooij (2004) reports a slight higher value: 2.9±0.28 wt.-%/b (normally distributed). This value is found for structures around the Dutch coast older than 10 years, up to a structure's height of 7 m +NAP, and made with BFS cement type. For higher heights, the conditions that hold for submerged structures no longer apply.

In Edvardsen and Mohr (1999) a similar value is proposed, although the variation is much larger: 2.33±1.18 wt.-%/b (normal distributed). However, more information on these parameters is still missing.

5.5 k-factors k_e, k_c, k_G

Environmental factor k_e

The rate at which chlorides diffuse is affected by the temperature of the solution (Gehlen, Greve-Dierfeld et al. 2015). The environmental factor k_e enables the diffusion coefficient to be applicable in different environmental conditions. k_e simplifies the thermodynamical processes to a single value.

For BFS cement in the submerged area, DuraCrete, Brite et al. (2000) propose a value of 3.88±1.29 (Gamma distributed). For PC cement they recommend taking a value of 1.33±0.22 (Gamma distributed) in the submerged zone. In general, BFS cement shows a significant higher mean value than PC. The spread is also larger. Table 5.3 summarizes the findings for the submerged, tidal and splash zone.

Table 5.3: Quantification of the environmental factor for OPC-concrete and BFS-concrete (table taken from DuraCrete, Brite et al. (2000))

Binder type	Environment	Distribution type	Mean	Standard deviation
OPC	Submerged	Gamma	1.325	0.223
OPC	Tidal	Gamma	0.924	0.155
OPC	Splash	Gamma	0.265	0.045
BFS	Submerged	Gamma	3.877	1.292
BFS	Tidal	Gamma	2.704[1]	1.292[1]
BFS	Splash	Gamma	0.777[1]	1.292[1]

[1] The rows marked in gray are quantified with expert opinion (DuraCrete et al., 2000)

Edvardsen and Mohr (1999) use a value of 0.92±0.16 (Gamma distributed) in the tidal area. This is in line with what DuraCrete, Brite et al. (2000) recommends for PC in that area. Since the mean values differ a lot between PC and BFS, Edvardsen and Mohr (1999) probably assumed a PC concrete structure.

Curing factor k_c

Some studies on the determination of k_c have been executed e.g., DuraCrete, Brite et al. (2000). These studies were limited and should be seen in relation to a reference value. That is why in other studies, people opted to take the curing factor equal to 1 and incorporate the variability in another parameter e.g., Edvardsen and Mohr (1999).

Combined environmental- and curing factor k_G

Gehlen (2000) groups all parts of a structure that are submerged or within the splash zone into a single category, assuming that structures in the splash zone are exposed to moisture so frequently that the influence of curing or drying is negligible. The atmospheric zone, which refers to parts of the structure above the splash zone that are only exposed to air and minimal direct water contact, is excluded from this group.

The result is that the k-factors can be combined into a single, new factor in this particular set. This factor is only depending on the environmental conditions (i.e., the temperature) Although Gehlen (2000) referred to this parameter as k_e again, we will name the combined parameter k_G in order to prevent confusions. He used the Arrhenius equation to describe k_G. The Arrhenius equation describes the temperature dependence of a chemical reaction and is presented in Eq. 40.

$$k_G = \exp\left[b_e\left(\frac{1}{T_{ref}} - \frac{1}{T_e}\right)\right]$$

Eq. 40

where:

- b_e is a regression parameter (K);
- T_{ref} is the reference temperature (293 K);
- T_e is the ambient temperature (K).

For b_e , Gehlen (2000) adopted a value of 4800±700 K (normal distributed).

This strategy is adopted by others. For example, Polder and de Rooij (2004), Gehlen, Greve-Dierfeld et al. (2015), JCSS (2020). Studies that contradict this method have not yet been found.

In Polder and de Rooij (2004), the suitability of using a subset is very noticeable. There, after excluding the measurements in the atmospheric zone, a linear regression yielded a coefficient of determination of $R^2 = 0.86$. When including the atmospheric data (data related to the state of the atmosphere in the vicinity of the structure), the coefficient of determination is $R^2 = 0.16$.

5.6 Age exponent α

The age exponent α is required to describe the time dependence of the chloride transport. It depends on the type of cement and the exposure conditions. A higher age exponent results in a higher diffusion coefficient.

In his research, Gehlen (2000) found that α can be described as 0.45±0.20 (beta distributed, $a = 0$, $b = 1$). This is, again, based on samples that were exposed to marine environments. The JCSS (2020) and *fib* Bulletin 34 (fib) also use this stochastic variable to describe α in case BFS binder is used.

Edvardsen and Mohr (1999) propose a value of 0.37±0.07 (beta distributed, $a = 0$, $b = 1$). As mentioned before, they show no evidence to support this distribution type and parameters. Section 5.5 presented evidence to believe Edvardsen and Mohr (1999) used PC in their calculation. For PC, JCSS (2020) and fib (2006) both suggest 0.30±0.12 (beta distributed, $a =$

$0, b = 1$) to describe α. This does not support the statement made in section 5.5, as their value is located in between PC and BFS.

Polder and de Rooij (2004) found a value of 0.48±0.07 (beta distributed, $a = 0, b = 1$), based on BFS samples in a marine environment. Compared to Gehlen (2000), Polder and de Rooij (2004) used a much smaller sample size (11 versus 112). Polder and de Rooij (2004) assumed that their data was also beta-distributed, which makes it unlikely that the sample size was properly taken into account. This would lead to a smaller standard deviation. However, this could also be the result of testing specimen that only come from the Dutch coast, which is a subgroup of the total population.

6 Discussion and Conclusions

Modeling chloride ingress in reinforced concrete structures is crucial for predicting durability and ensuring long-term safety, particularly in structures exposed to marine environments. Chloride ingress modeling seeks to represent complex physical and chemical processes that influence the onset and progression of corrosion in concrete. According to DuraCrete (1998), a comprehensive model for chloride ingress should address multiple stages, including the time-dependent ingress of chlorides, the corrosion initiation threshold, reduction of cover depth, corrosion rate, and the resulting structural impacts. However, achieving an accurate model for each of these stages is challenging due to various influencing factors (Section 4.3.1 and 4.3.2) and the complexity of the corrosion process.

Modeling chloride ingress and corrosion propagation in reinforced concrete structures is challenging due to the complex variability of key parameters and their mutual dependence, like the chloride threshold and corrosion rate. The chloride threshold (beyond which chloride concentration causes the passive layer on reinforcing steel to deteriorate) varies significantly with factors like concrete mix, compaction quality, cover depth, and environmental exposure. Similarly, the corrosion rate, which defines how quickly the reinforcement deteriorates once corrosion initiates, depends on parameters such as the water-cement (w/c) ratio, ambient temperature, concrete microstructure and the hydrothermal conditions in the interface steel/concrete.

These factors are well-documented, but it is difficult to select which variables most significantly impact the chloride threshold and corrosion rate. This is because their effects vary based on local environmental conditions and structure-specific characteristics. Consequently, the resulting uncertainty in model predictions complicates the accurate evaluation of structural durability.

The initiation phase models predict the time until chloride concentrations reach the critical threshold at the steel surface, initiating corrosion. This phase is complex due to various influential factors, including concrete composition, cover depth, exposure conditions, and chloride sources. Empirical models, often based on Fick's second law of diffusion, approximate chloride ingress using a diffusion coefficient that varies with concrete age and exposure conditions. However, these models are limited because they need data from inspected structures, which may not represent all environmental or structural conditions.

In the propagation phase (following corrosion initiation) the durability and service life of RC structures are significantly impacted. While the model presented by Tuutti (1982) divides service life into initiation and propagation phases, it does not cover the sub-phases of propagation in detail. Factors such as w/c ratio, chloride concentration, temperature, and moisture content in concrete, affect the corrosion rate differently. This phase concludes when structural performance degrades to a predefined limit state indicating by loss of steel cross-section, reduced stiffness or bond strength, or cracking of the concrete cover.

While most models emphasize the initiation phase of corrosion, it is important to consider the corrosion propagation phase, although in this report was addressed briefly, to understand the full impact of chloride ingress on structural durability. After the initiation of corrosion, chloride-induced degradation accelerates due to the formation of expansive corrosion products, which induce cracking and spalling in the concrete cover. Although some empirical models touch upon corrosion propagation by estimating corrosion rates after initiation, there remains a need for more comprehensive models that account for both initiation and propagation in an integrated manner, particularly for long-term durability assessments. A separate report details on a modelling proposal that combines both corrosion stages.

Conclusions

In this report, a comprehensive literature review and state of the art predictive models for estimating the remaining service life of concrete structures in marine environments, with a particular focus on chloride-induced corrosion during both the initiation and propagation phases.

A key insight from examining these methodologies is the role of condition limit states in reducing uncertainties associates with service life conditions. The report shows the differences between various models, particularly empirical models that address the initiation phase of corrosion. These models, which consider the time-dependent diffusion coefficient, surface chloride concentration, and other age-related variables, are crucial for accurately predicting chloride ingress in concrete. However, their reliance on simplified assumptions, such as constant environmental conditions and uniform material properties, limits their applicability to idealized scenarios.

It was found that there is significant variability in chloride ingress due to material, structural, and environmental factors, with studies like DuMaCon (Polder and de Rooij 2004) showing that uncertainty can be minimized by focusing on specific concrete types, element locations, and exposure conditions. For example, the critical chloride threshold for Blast Furnace Slag cement, commonly used along the Dutch coast, is approximately 0.5 wt.-%/binder.

The models reviewed in this report are primarily valid for non-cracked concrete conditions. The effects of cracking, bond strength degradation, and other deterioration mechanisms have not been considered in detail, which may limit the scope of the findings when applied to damaged or aging structures. Additionally, the variability in chloride ingress due to fluctuating environmental conditions, such as tidal variations and seasonal changes, remains a critical area for further exploration. Future work should focus on incorporating field data, such as chloride profiles, environmental conditions, and inspection results, to validate the methodologies.

This literature review provides a basis for reliability-based service lifetime calculations. The details of this reliability-based framework are further explained in a separate report.

7 References

Andrade, C., J. Díez and C. Alonso (1997). Modelling of skin effects on diffusion process in concrete. Proceedings of the RILEM International Workshop on Chloride Penetration into Concrete (182-194). Paris.
Bamforth, P. B. (1994). "Admitting that chlorides are admitted." Concrete **28**(6).
Bamforth, P. B. (1995). A new approach to the analysis of time-dependent changes in chloride profiles to determine effective diffusion coefficients for use in modelling of chloride ingress. RILEM International Workshop on Chloride Penetration into Concrete, RILEM Publications SARL, Paris, France.
Bamforth, P. B. (1999). "The derivation of input data for modelling chloride ingress from eight-year UK coastal exposure trials." Magazine of Concrete Research **51**(2): 87-96.
Bjegović, D., V. Krstić and D. Mikulić (2006). "Design for durability including initiation and propagation period based on the fuzzy set theory." Materials and Corrosion **57**: 642 - 647.
Breit, W. (2001). "Kritischer korrosionsauslösender Chloridgehalt-Sachstand und neuere Untersuchungen." Betontechnische Berichte; Concrete Technology Reports: VBT Verlag Bau u. Technik: 145-168.
Browne, R. (1982). "Design prediction of the life for reinforced concrete in marine and other chloride environments." Durability of building materials **1**: 113-125.
Burggraaf, H .G. (2022a). TNO 2022 R10416 Betononderzoek Hartelkering.
Burggraaf, H .G. (2022b). TNO 2022 R10417 Betononderzoek Hollandsche IJsselkering.
Burggraaf, H .G. (2022c). TNO 2022 R10418 Betononderzoek Maeslantkering.
Chun-Qing, L., R. E. Melchers and Z. Jian-Jun (2006). "Analytical model for corrosion-induced crack width in reinforced concrete structures." ACI structural journal **103**(4): 479.
Crank, J. (1979). The mathematics of diffusion, Oxford university press.
CUR (2009). Leidraad 1, Durability of structural concrete with regard to chloride induced reinforcement corrosion - Guideline for formulating performance requirements (in Dutch).
CUR (2018). CUR-Aanbeveling 121:2018 Bepaling ondergrens verwachte restlevensduur van bestaande gewapende betonconstructies (in Dutch).
DuraCrete (1998). "Modelling of degradation, DuraCrete–Probabilistic performance based durability design of concrete structures." EU-BriteEuRam III, Contract BRPR-CT95-0132, Project BE95-1347/R4-5: 174.
DuraCrete (2000). R17 Final Technical Report.
DuraCrete, E. Brite, III and R. Civieltechnisch Centrum Uitvoering Research en (2000). Statistical quantification of the variables in the limit state functions : DuraCrete, probabilistic performance based durability design of concrete structures. [Gouda], [CUR] [Gouda].
Edvardsen, C. and L. Mohr (1999). "DURACRETE–a guideline for durability-based design of concrete structures." Prague, October.
fib (2006). fib bulletin 34-Model Code for Service Life Design. F. I. d. Béton, Lausanne.
Funahashi, M. (1990). "Predicting corrosion-free service life of a concrete structure." ACI Mater. J **87**: M62.
Gehlen, C. (2000). "Probabilistische Lebensdauerbemessung von Stahlbetonbauwerken. Deutscher Ausschuss für Stahlbeton, Heft 510." Beuth, Berlin.
Gehlen, C., S. v. Greve-Dierfeld, J. Gulikers, S. Helland and A. Rahimi (2015). "fib Bulletin 76: Benchmarking of Deemed-to-Satisfy Provisions in Standards–Durability of Reinforced Concrete Structures Exposed to Chlorides."

Izquierdo, D., C. Alonso, C. Andrade and M. Castellote (2004). "Potentiostatic determination of chloride threshold values for rebar depassivation: experimental and statistical study." Electrochimica Acta **49**(17-18): 2731-2739.
Jensen, O. M., P. F. Hansen, A. M. Coats and F. P. Glasser (1999). "Chloride ingress in cement paste and mortar." Cement and Concrete Research **29**(9): 1497-1504.
Li, C. Q. (2004). "Reliability Based Service Life Prediction of Corrosion Affected Concrete Structures." Journal of Structural Engineering **130**(10): 1570-1577.
Luping, T. and L.-O. Nilsson (1993). "Chloride Penetration into Concrete Structures — Nordic Miniseminar." Division of Building Materials, Chalmers University of Technology, Publication P-93:1.
Maage, M., S. Helland and J. E. Carlsen (1995). Practical non-steady state chloride transport as a part of a model for predicting the initiation period. Proceedings of the 1st International RILEM Workshop.
Mangat, P. and B. Molloy (1994). "Prediction of long term chloride concentration in concrete." Materials and structures **27**: 338-346.
Martın-Pérez, B. (1999). Service life modelling of RC higway structures exposed to chlorides, University of Toronto Toronto, ON, Canada.
Mejlbro, L. (1996). "The complete solution of Fick's second law of diffusion with time-dependent diffusion coefficient and surface concentration." Durability of concrete in saline environment: 127-158.
Neville, A. (1995). "Chloride attack of reinforced concrete: an overview." Materials and Structures: 63-70.
Nieves-Mendoza, D., C. Gaona-Tiburcio, H. L. Hervert-Zamora, R, P. Castro-Borges, R, P. Z. Robledo, A. Martínez-Villafañe and F. Almeraya-Calderón (2012). "Statistical Analysis of Factors Influencing Corrosion in Concrete Structures." International Journal of Electrochemical Science **7**(6): 5495-5509.
Nilsson, L.-O., Poulsen, E., Sandberg, P., Sørensen, H., and Klinghoffer, O. (1996). HETEK, Chloride penetration into concrete, State-of-the-Art. Transport processes, corrosion initiation, test methods and prediction models.
Otieno, M. B., M. G. Alexander and H. D. Beushausen (2010). "Corrosion in cracked and uncracked concrete – influence of crack width, concrete quality and crack reopening." Magazine of Concrete Research **62**(6): 393-404.
Pacheco, J. and R. Polder (2016). "Incorporating cracking of concrete on chloride ingress and service life modeling of concrete structures." Proceedings of Corrosion 2016; Collaborate, Educate, Innovate, Mitigate.Pacheco, J. and R. Polder (2016). "Incorporating cracking of concrete on chloride ingress and service life modelling of concrete structures."
Polder, R. B. and Rooij, M. R. de (2004). Duurzaamheid Mariene Constructies (DuMaCon). Eindrapport CUR-Onderzoekscommissie B82, TNO**:** 105.
Polder, R. B. and Rooij, M. R. de (2005). Durability of marine concrete structures – field investigations and modelling, HERON, Vol. 50 (3), 133-143
Poulsen, E. (1993). On a model of chloride Ingress into concrete having time dependent diffusion coefficient, Chalmers Tekniska högskola, P-93: 1. Proc. Chloride Penetration into Concrete Structure, Nordic Mini Seminar, edit. Lars-Olof Nilsson, Göteborg.
Poulsen, E. (1995). Design of rebar concrete covers in marine concrete structures deterministic approach. Proceedings of International RILEM workshops, LO Nilsson and JP Ollivier, edns., RILEM, Cachon Cedex, France.
Rasheeduzzafar, S. Al-Saadoun and A. Al-Gahtani (1992). "Corrosion cracking in relation to bar diameter, cover, and concrete quality." Journal of Materials in Civil Engineering **4**(4): 327-342.
Raupach, M. (1996). "Chloride-induced macrocell corrosion of steel in concrete—theoretical background and practical consequences." Construction and building materials **10**(5): 329-338.
Rodríguez, J., C. Andrade and G. Somerville (2002). "Manual for assessing corrosion-affected concrete structures." Geocisa and Torroja Institute, EC Innivation Programme, IN30902I.

Scott, A. and M. G. Alexander (2007). "The influence of binder type, cracking and cover on corrosion rates of steel in chloride-contaminated concrete." Magazine of Concrete Research **59**(7): 495-505.
Sobhani, J. and A. Ramezaninpour (2009). Modeling the corrosion of reinforced concrete structures based on fuzzy systems. Proceedings of the 3rd International Conference on Concrete and Development.
Stansbury, E. E. and R. A. Buchanan (2000). Fundamentals of electrochemical corrosion. Materials Park, OH, ASM International.
Tang, L. and L. Nilsson (2018). "10 SERVICE LIFE PREDICTION FOR CONCRETE STRUCTURES UNDER SEAWATER BY A NUMERICAL APPROACH." Durability of Building Materials & Components 7 vol. 1: 97.
Tumidajski, P., G. Chan, R. Feldman and G. Strathdee (1995). "A Boltzmann-Matano analysis of chloride diffusion." Cement and concrete research **25**(7): 1556-1566.
Tuutti, K. (1982). Corrosion of steel in concrete.
Warkus, J., M. Brem and M. Raupach (2006). "BEM-models for the propagation period of chloride induced reinforcement corrosion." Materials and Corrosion **57**(8): 636-641.
Xia, P.-Q. and J. M. W. Brownjohn (2003). "Residual stiffness assessment of structurally failed reinforced concrete structure by dynamic testing and finite element model updating." Experimental Mechanics **43**(4): 372-378.
Zhu, J. (2013). The finite element method: its basis and fundamentals, Elsevier.
Živica, V. (2003). "Influence ofw/c ratio on rate of chloride induced corrosion of steel reinforcement and its dependence on ambient temperature." Bulletin of Materials Science **26**(5): 471-475.

Mobility & Built Environment

Molengraaffsingel 8
2629 JD Delft
www.tno.nl

TNO innovation for life